TECHNICAL ADVANCES AND RESOURCES

Rapid identification and characterization of infected cells in blood during chronic active Epstein-Barr virus infection

Benjamin Fournier[1,2], David Boutboul[3], Julie Bruneau[2,4], Charline Miot[5], Cécile Boulanger[6], Marion Malphettes[3], Isabelle Pellier[5], Bertrand Dunogué[7], Benjamin Terrier[7], Felipe Suarez[8], Stéphane Blanche[9], Martin Castelle[9], Sarah Winter[9], Henri-Jacques Delecluse[10], Thierry Molina[2,4], Capucine Picard[1,2,11], Stephan Ehl[12], Despina Moshous[2,9], Lionel Galicier[3], Vincent Barlogis[13], Alain Fischer[2,9,14,15], Bénédicte Neven[2,9], and Sylvain Latour[1,2]

Epstein-Barr virus (EBV) preferentially infects epithelial cells and B lymphocytes and sometimes T and NK lymphocytes. Persistence of EBV-infected cells results in severe lymphoproliferative disorders (LPDs). Diagnosis of EBV-driven T or NK cell LPD and chronic active EBV diseases (CAEBV) is difficult, often requiring biopsies. Herein, we report a flow-FISH cytometry assay that detects cells expressing EBV-encoded small RNAs (EBERs), allowing rapid identification of EBV-infected cells among PBMCs. EBV-infected B, T, and/or NK cells were detectable in various LPD conditions. Diagnosis of CAEBV in 22 patients of Caucasian and African origins was established. All exhibited circulating EBV-infected T and/or NK cells, highlighting that CAEBV is not restricted to native American and Asian populations. Proportions of EBV-infected cells correlated with blood EBV loads. We showed that EBV-infected T cells had an effector memory activated phenotype, whereas EBV-infected B cells expressed plasma cell differentiation markers. Thus, this method achieves accurate and unambiguous diagnoses of different forms of EBV-driven LPD and represents a powerful tool to study their pathophysiological mechanisms.

Introduction

The EBV is an oncogenic virus of the Herpesviridae family restricted to humans with a selective tropism for epithelial cells and B lymphocytes. EBV is implicated in a range of cancers, including gastric and nasopharyngeal carcinomas, smooth muscle tumors, B cell neoplasms such as Hodgkin lymphoma, diffuse large B cell lymphoma, Burkitt lymphoma, and T and natural killer (NK) cell lymphomas. EBV infection is the first known risk of cancer-associated mortality in emerging countries (Young and Rickinson, 2004; Plummer et al., 2016).

EBV infects all human populations, with more than 90% being carriers by the age of 20 yr. In immunocompetent individuals,

EBV establishes long-term persistent asymptomatic infection of B cells. However, during the primary infection, some individuals develop infectious mononucleosis (IM), a clinical manifestation that reflects a strong but self-limiting immune response without persistent deleterious consequences. In immunocompromised subjects, EBV infection is associated with life-threatening pathologies such as hemophagocytic lymphohistiocytosis (HLH) and B cell lymphoproliferative disorders (B-LPD), including lymphomas. These disorders are observed in HIV-infected patients with AIDS and in patients receiving immunosuppressive treatments following organ transplantation, usually denoted as

post-transplant lymphoproliferative disorders (PTLDs). Patients with inherited immunodeficiencies are also prone to develop EBV-related B-LPD. In particular, there is a subgroup of primary immunodeficiencies (PIDs) characterized by a high and specific predisposition to EBV infection and to development of EBV-related B-LPD. These PIDs are caused by autosomal recessive or X-linked mutations in genes required for the expansion and cytotoxic responses of EBV-specific T cells (Latour and Winter, 2018; Tangye et al., 2017; Latour and Fischer, 2019). Most of these conditions logically respond to depletion of the EBV reservoir in B cells by anti-CD20 antibodies such as rituximab.

More rarely, EBV infection is associated with T and NK lymphoproliferative diseases (T/NK-LPDs), in which EBV infects T or NK cell subsets. T/NK-LPDs include malignant (i.e., extranodal NK/T lymphoma [ENKTL]) and the nonmalignant conditions (i.e., T and NK cell chronic active EBV infection diseases [CAEBV]; Swerdlow et al., 2016; Kim et al., 2019). CAEBV infections are further divided into systemic and cutaneous forms (i.e., severe mosquito bite allergy and hydroa vacciniforme–like LPD; Quintanilla-Martinez et al., 2013; Cohen et al., 2019).

T/NK-LPD and CAEBV have been mostly reported in native populations from Asia and the Americas (Quintanilla-Martinez et al., 2013; Kimura et al., 2012). Their etiology is poorly understood, but polygenic factors and immune defects are thought to favor their occurrence. Along these lines, somatic mutations in DDX3X have been shown to play a role in the progression of the disease (Okuno et al., 2019). Furthermore, we recently identified a familial form of systemic T cell CAEBV caused by digenic homozygous loss-of-function mutations in TNFRSF9 (4-1BB/CD137) and PIK3CD resulting in defective immune control of EBV-infected T cells (Rodriguez et al., 2019).

One common feature of T/NK-LPD is the high EBV load in the blood of patients that is not relieved by anti-CD20 treatment and can persist for years. The persistence of EBV-infected T cells and/or NK cells may progress to life-threatening LPDs often associated with HLH. In contrast to B-LPD, these conditions have a poor prognosis (Kim et al., 2016; Kimura et al., 2012; Kawamoto et al., 2018). Indeed, they are often refractory to standard treatments, and although hematopoietic stem cell transplantation (HSCT) represents the best curative therapy so far, management remains difficult and differs from that of B-LPD (Sawada and Inoue, 2018; Bollard and Cohen, 2018; Sawada et al., 2017).

Most T/NK-LPDs, including CAEBV-related diseases, are not familiar to clinicians because of their relative rarity and have misleading and various clinical presentations that may impede the diagnosis. They range from chronic lymphoid organ enlargement and overt autoinflammatory diseases to unexplained recurrent and/or fulminant HLH. So far, the presence of EBV in T or NK cells has been mostly obtained by immunostaining of biopsies or by PCR of sorted cells. Both assays can be difficult to perform and give ambiguous results. Even when CAEBV is suspected (especially in case of a poor clinical and biological response to B cell depletion), reaching an accurate diagnosis may be hampered by the absence of any lesions to analyze or by a poor clinical

condition that may prevent any invasive organ biopsy. However, providing an accurate and rapid diagnosis by showing EBV-infected T and/or NK cells is key to adjust the treatment. The lack of direct access to infected cells also restrains progress in the understanding of mechanisms underlying the pathophysiology of these diseases, which is so far largely not understood.

We report a minimally invasive, rapid method allowing reliable detection and characterization of EBV-infected cells from peripheral blood mononuclear cells (PBMCs). We showed the suitability of this test to diagnose EBV-driven T/NK-LPD and to study EBV-infected cells.

Results

Detection of EBV-infected cell lines using a flow cytometry RNA assay

We developed a fluorescence in situ hybridization (FISH) flow cytometry (flow-FISH) method that detects EBER-1 and EBER-2 mRNAs (EBERs) expressed by EBV based on the PrimeFlow RNA assay (Henning et al., 2016). After cell fixation and permeabilization, EBERs are recognized through hybridization with a specific oligonucleotide probe, which is then serially hybridized with two specific DNA probes to amplify the signal, the last one being fluorescent. Importantly, EBERs are expressed in all EBV-containing cells, irrespective of the lytic and latency programs (Lerner et al., 1981). To assess the specificity of the assay, several known EBV-positive (EBV+) and EBV-negative (EBV−) cell lines were tested, including two EBV+ and EBV− Burkitt lymphoma cell lines (Raji: EBV+; Ramos: EBV−), human B cells immortalized with EBV in vitro (termed "LCL" for lymphoblastoid cell line), an EBV+ NK cell line (SNK-6), an EBV− T cell leukemia (Jurkat) cell line, and the human embryonic kidney HEK-293 cell line, stably infected or not with a GFP-tagged EBV (HEK and EBV-GFP+HEK; Delecluse et al., 1998). Cell lines were also tested with Bacillus and RLP13A probes as a control (Fig. 1 A). The Bacillus probe targets a bacterial RNA that is not expressed in human cells and is used to assess background staining, whereas the RPL13A probe recognizes a ubiquitous human ribosomal RNA present in all cell types and served as a positive control. Both EBER and Bacillus probes are coupled to the fluorochrome Alexa Fluor 647, whereas the RPL13A probe is coupled to the fluorochrome Alexa Fluor 488. All cells were incubated with a viability dye (eFluor 450 dye), and only eFluor-negative cells were analyzed. All cell lines known to contain EBV (Raji, SNK-6, LCL, and EBV-GFP+ HEK) showed more than 90% of cells positively stained with the EBER probe. In contrast, cells known not to be infected by EBV (HEK, Ramos, and Jurkat) exhibited a very low percentage of EBER+ cells. These latter can be viewed as false-positive background because their frequency was similar to or below that of cells stained with the Bacillus probe and because both stains had a low mean fluorescence intensity (MFI). Of note, in some experiments, we noticed that a proportion of LCL was negative for EBER. EBER expression was shown to be downregulated during the switch from viral latency to lytic cycle (Greifenegger et al., 1998) and to be negative in epithelial cells from hairy leukoplakia, in which EBV infection is
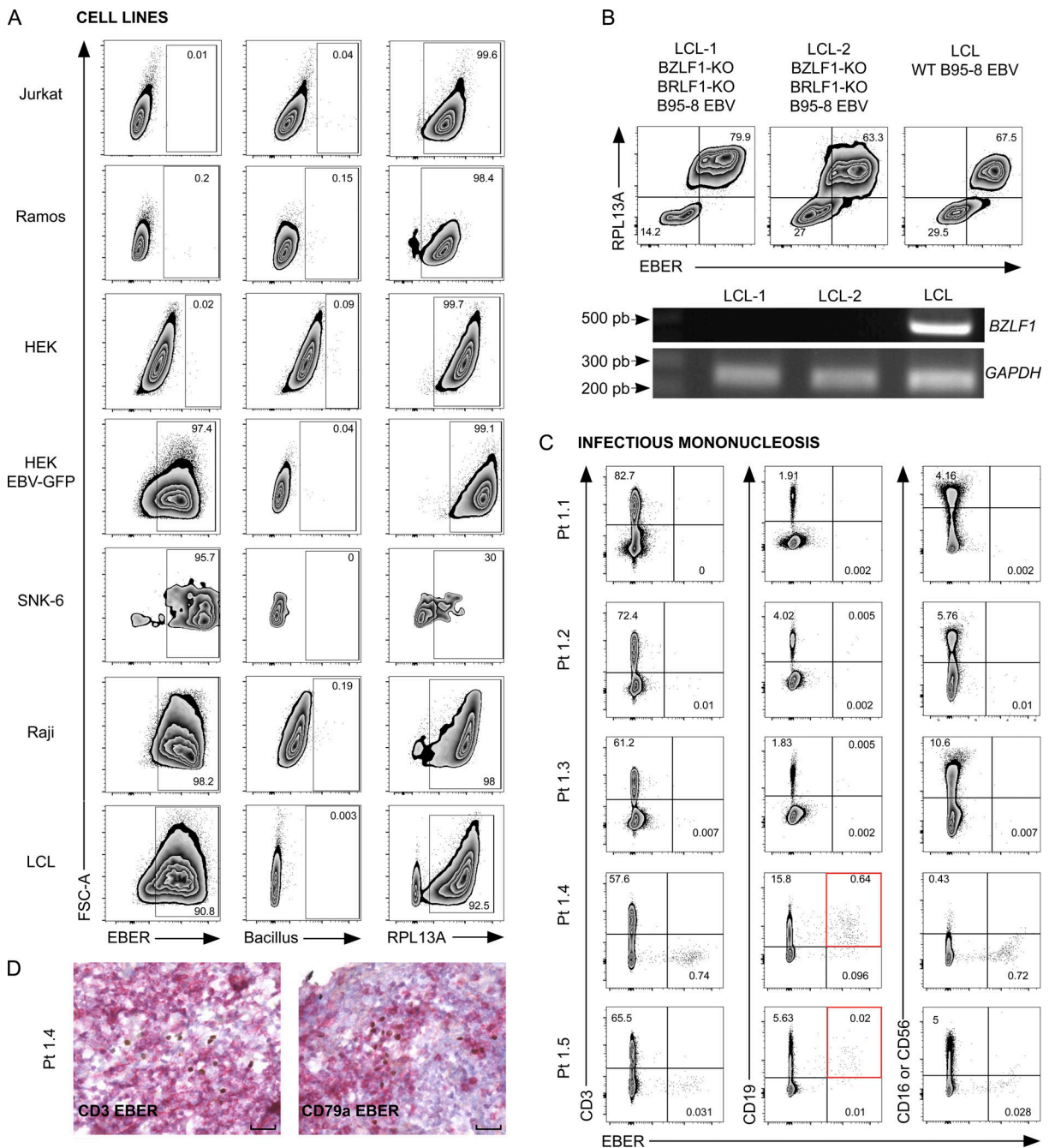
Fournier et al.
Detection of circulating EBV-infected cells

Journal of Experimental Medicine   2 of 20
https://doi.org/10.1084/jem.20192262

Figure 1. PrimeFlow assay for EBER allows specific detection of EBV-containing cell lines and circulating EBV-infected B cells during severe IM.
(A) FACS dot plots of EBER (left panels), Bacillus (middle panels), and RPL13 (right panels) stains using the PrimeFlow RNA assay of EBV⁻ cell lines (Jurkat, Ramos, and HEK) and EBV⁺ cell lines (HEK EBV-GFP, SNK-6, Raji, and LCL). The Bacillus probe targets a bacterial RNA, whereas the RPL13A probe targets a ubiquitously expressed ribosomal RNA, and they are used as negative and positive controls, respectively. The RPL13A probe is coupled to the fluorochrome Alexa Fluor 488, except for the analysis of HEK GFP-EBV, for which it is coupled to Alexa Fluor 647. **(B)** Upper panels show FACS dot plots of costaining with RPL13A and EBER probes (coupled to Alexa Fluor 488 and 647, respectively) of LCL cells treated for 72 h with TPA + ionomycin stimulation to induce the lytic cycle. LCL-1 and LCL-2 lines were obtained by infection with the BZLF1-KO BRLF1-KO B95-8 EBV strain and devoid of the essential BLZF1 and BRLF1 proteins required to induce the EBV lytic cycle. LCL cells were obtained by infection with the B95-8 EBV WT strain (WT B95-8 EBV). Lower panels show expression of BZLF1 (453 pb) and GAPDH (258 pb) fragment transcripts by RT-PCR in TPA + ionomycin–treated LCL-1, LCL-2, and LCL cell lines. GAPDH was used as an amplification control and DNA ladder (pb) on the left. **(C)** FACS dot plots of EBER expression by the PrimeFlow assay coupled with anti-CD3, anti-CD19, anti-CD16, or anti-CD56 staining of PBMCs from patients with IM. Dot plots are gated on eFluor⁻ CD14⁻ cells. The red gates in the dot plots highlight the EBV-infected cell subsets. Patients (Pt) 1.1, 1.2, and 1.3 had mild IM symptoms and low plasma EBV loads. Pt 1.4 and Pt 1.5 had severe IM symptoms and high plasma EBV loads. **(D)** Tonsil biopsy section from Pt 1.4 that has been costained with an EBER probe and anti-CD3 or anti-CD79a antibodies, showing infiltration of EBV-infected B cells in tissues. Magnification, ×400. Scale bars, 40 µm.

considered to be purely lytic (Gilligan et al., 1990). To assess if the EBER-negative LCL cells could correspond to cells with EBV in the lytic program, the EBV lytic cycle was induced by 12-O-tetradecanoylphorbol-13-acetate (TPA) and ionomycin in WT LCL cells (infected with the EBV strain B95-8) or LCL cells that were obtained by infection with a defective B95-8 strain lacking *BZLF1* and *BRLF1*, two viral factors required for EBV to undergo the lytic cycle (Feederle et al., 2000; Fig. 1 B). Although lytic cycle induction was detectable by BZLF1 expression by RT-PCR in WT LCL treated with TPA and ionomycin, no BZLF1 expression was found in *BZLF1/BRLF1* double-deficient LCL, as expected. However, in all conditions, EBER-negative cells were not stained with the RPL13A-positive control probe, indicating that they likely have not been permeabilized or hybridized with the probes rather than being true-negative cells. These data also suggest that when the EBV lytic cycle is activated in B cells, there is enough EBER expression to be detected with the PrimeFlow assay. These findings are in line with recent evidence of increased EBER1/2 expression in LCL after EBV lytic cycle induction (Li et al., 2019).

PrimeFlow was then used in patients with proven EBV-driven B-LPD and T/NK-LPD by histology. Analysis was further extended to patients in whom standard histology was not performed (16 of 39), either because clinical and biological context was sufficient for a conclusive diagnosis (i.e., IM and hydroa vacciniforme–like LPD) or because no lesion was available to biopsy. More details related to clinical manifestations and histology of patients are reported in Table 1. Analyses of infected subsets were performed after the exclusion of dead cells (eFluor+) and monocytes (CD14+), for which the absence of EBER+ was systematically verified.

Detection of EBV-infected circulating cells from PBMCs of healthy individuals and patients with EBV-driven B-LPD

We tested whether the PrimeFlow EBER assay could enable the detection and phenotyping of EBV-infected cells among PBMCs of EBV-infected healthy individuals and patients. In all following experiments, 1.5 million to 3 million PBMCs were tested. First, we verified that conditions for intracellular hybridization with the EBER probe did not alter extracellular costaining with antibodies to common specific markers of monocytes and B, T, and NK cell populations. The distributions of the different lymphocyte subsets within PBMCs from healthy individuals (including B lymphocytes; CD3, CD4, CD8, and γδ T lymphocytes; NK cells; and monocytes) were comparable to those obtained under classic conditions, even though the MFI of each marker was slightly reduced when we used the PrimeFlow protocol (Fig. S1 and data not shown). Naive and memory T and B cell phenotypes were also found to be comparable (data not shown). No difference was noticed between fresh and frozen samples (data not shown). Tested antibodies suitable for the PrimeFlow EBER assay are listed in Table S1. We then analyzed PBMCs from 15 healthy control subjects, including both EBV-seronegative (3 individuals) and EBV-seropositive (12 individuals) subjects (Fig. S1, Fig. 7 A, and data not shown). When costained with the EBER probe and antibodies for membrane markers, only few cells were positive (<0.05%) in PBMCs of all individuals tested,

irrespective of their EBV status. Proportions of EBER+ cells were always below the threshold of Bacillus-positive cells, and the very few positive cells in some control subjects were distributed across all lymphocyte subsets (in contrast to patients with B-LPD and T/NK-LPD shown in Figs. 2, 3, 4, 5, and 6; data not shown). These results strongly support that these few EBER+ cells represent false-positive cells.

We next tested PBMCs of patients diagnosed with IM (Fig. 1 C). Compared with the Bacillus probe staining (negative control probe; Fig. S2), no significant EBER+ cells were detected in any cell subset from PBMCs of three patients (patients [Pt] 1.1, 1.2, and 1.3) who had low detectable blood EBV loads by PCR (ranging from 2.6 to 2.9 log copies/ml). This may be explained by the fact that symptoms of IM result from a strong expansion of EBV-specific T cells and/or NK cells, a time at which most EBV-infected B cells may already have been eliminated (Balfour et al., 2005; Hadinoto et al., 2008). In contrast, significant amounts of EBER+ cells restricted to CD19+ cells were detected in two patients (Pt 1.4 and 1.5) diagnosed with more severe symptoms related to IM (Fig. 1 C) and high EBV loads (5 and 6.2 log copies/ml, respectively). No other positive cells were found among other lymphoid cell subsets. This specific B cell EBER staining was in accordance with EBER and CD79a costaining in standard histology of a lymph node biopsy from Pt 1.4 (Fig. 1 D).

Patients with EBV-associated B-LPD were further examined, including patients with solid B cell neoplasia (Hodgkin lymphoma, n = 3; PTLD, n = 1; Fig. 2 A), inherited immune deficiencies predisposing to EBV-driven B-LPD, such as X-linked lymphoproliferative syndrome type 1 (XLP-1; n = 2), CD70 deficiency (Izawa et al., 2017), MAGT1 deficiency (Li et al., 2011), and CTPS1 deficiency (Martin et al., 2014, 2020), or not particularly predisposing to EBV like the combined ZAP-70 immunodeficiency (Fig. 2 B). No significant EBV+ circulating cells were detected in PBMCs from two patients with EBV+ Hodgkin lymphoma, despite positive blood EBV load in one of them. The third patient with Hodgkin lymphoma had very rare EBER+ cells in the B cell subset (0.29% of B cells). Patients with PTLD following liver transplant and those with CD70, CTPS1, and ZAP-70 deficiencies all had high chronic EBV load and exhibited between 0.4% and 3.5% EBV+ B cells (n = 4). Of note, only the CD70-deficient patient had signs of LPD. A MAGT-1–deficient patient was tested during primary EBV infection based on EBV serology and presented a low proportion of EBV+ cells (0.1%). Both XLP-1 patients had B cell lymphocytosis during a fulminant IM-like episode with a high proportion of EBER+ cells restricted to B cells (between 33.9% and 20.5% among PBMCs). The specific B cell EBER staining was in agreement with EBER probe and anti-CD79a costaining on the formalin-fixed, paraffin-embedded liver biopsy from Pt 2.10 (XLP-1; Fig. 2 C). These data demonstrate the reliability of the PrimeFlow EBER assay for achieving specific detection of circulating EBV-infected B cells in a range of pathological conditions in which EBV infection is known to drive B-LPD.

Detection of EBV-infected circulating cells among PBMCs of patients with post-transplant T-LPD and T/NK cell lymphoma

We next tested whether this assay could also be useful to characterize EBV-associated lymphoproliferations that likely

Fournier et al.
Detection of circulating EBV-infected cells

Journal of Experimental Medicine   4 of 20
https://doi.org/10.1084/jem.20192262

Table 1. **Characteristics of patients**

Patient	Ethnicity/origin	Age at onset (yr)	Clinical manifestations/genetic defects	PrimeFlow: EBV⁺ subset	Histology: EBV⁺ subset
IM					
Pt. 1.1	Caucasian	26	IM	Absent	NP
Pt 1.2	Caucasian	13	IM	Absent	NP
Pt 1.3	Caucasian	32	IM	Absent	NP
Pt 1.4	Sub-Saharan African	8	Severe IM (SMG and compressive lymph nodes requiring ventilation support)	CD19⁺	Tonsils and lymph node, CD79a⁺
Pt 1.5	Caucasian	23	Severe IM (SMG, thrombopenia)	CD19⁺	NP
B cell LPD					
Pt 2.1	North African	7	Classical Hodgkin lymphoma	Absent	Lymph node CD30⁺CD15⁺
Pt 2.2	Caucasian	26	Classical Hodgkin lymphoma	Absent	Lymph node (EBER not performed)
Pt 2.3	Sub-Saharan African	17	Classical Hodgkin lymphoma, HLH	CD19⁺	Lymph node CD30⁺CD15⁺
Pt 2.4	Caucasian	1	Liver transplantation, PTLD, high peripheral EBV load	CD19⁺	NP
Pt S4	North African	5	Fulminant IM	CD19⁻/low	Lymph node, CD79a⁺
Genetically characterized PIDs					
Pt 2.5	North African	8	B-cell LPD, HMG, SMG, ADP, CD70 deficiency (*TNFSF7* hmz mutation: c.535C>T/p.R179X)	CD19⁺	Lymph node, spleen, CD79a⁺
Pt 2.6	Comorian	14	Chronic peripheral EBV load without clinical LPD, ZAP-70 deficiency (*ZAP70* hmz mutation: c.252C>G/p.C84W), strongly decreased protein expression	CD19⁺	NP
Pt 2.7	Caucasian	3	Chronic peripheral EBV load without clinical LPD, CTPS1 deficiency (*CTPS1* hmz mutation: c.1692-1G>C/p.T566Dfs26X)	CD19⁺	NP
Pt 2.8	Caucasian	5	Primary EBV infection (ongoing), chronic hypogammaglobulinemia, MAGT1 deficiency (*MAGT1* hmz mutation: c.991C>T/p;R331X), strongly decreased protein expression	CD19⁺	NP
Pt 2.9	Caucasian	16	Fulminant IM, XLP-1 (*SH2D1A* hemiZ mutation: c.257-264delCATTTCAG p.A86EfsX15)	CD19⁺	Liver, CD79a⁺
Pt 2.10	North-African	9	Fulminant IM, XLP-1 (*SH2D1A* hemizygous exons 1-4 deletion)	CD19⁺	NP
T cell PTLDs					
Pt 3.1	Caucasian	2	HSCT for AML, persistent peripheral EBV load after rituximab	CD3⁺	NP
Pt 3.2	Caucasian	7	Cardiac transplantation, persistent peripheral EBV load after rituximab, hepatosplenomegaly, enlarged lymph nodes	CD8⁺	NP
Pt 3.3	Caucasian	2	Liver transplantation, persistent peripheral EBV load after rituximab, IBD	CD8⁺	Liver, bone marrow, gut CD8⁺
T/NK cell lymphomas					
Pt 3.4	Caucasian	15	ENKTL, nasal type	Absent	Nasal cavity, CD3⁺CD5⁻CD56⁺
Pt 3.5	Caucasian	60	Angioimmunoblastic T cell lymphoma revealed by EBV⁺ LPD, eosinophilia with lung involvement	CD3⁻CD4⁺	Lymph node, CD3⁺CD4⁺
Pt 3.6	Caucasian	74	ENKTL, recurrent HLH	CD3⁻CD56⁺	Skin, CD3⁺GrB⁺
Pt 3.7	Sub-Saharan African	33	ENKTL, HMG-SMG, bicytopenia, weight loss, fever	CD3⁻CD16⁺	Spleen, CD3⁺CD5⁻GrB⁻

Table 1. **Characteristics of patients (Continued)**

Patient	Ethnicity/origin	Age at onset (yr)	Clinical manifestations/genetic defects	PrimeFlow: EBV⁺ subset	Histology: EBV⁺ subset
Pt 3.8	North-African	43	Disseminated ENTKL, nasal type, recurrent fever and skin rashes, asymptomatic nasal cavity involvement (on biopsy)	CD3⁻CD16⁺	Skin, nasal cavity, CD16⁺CD56⁻
CAEBV, systemic EBV-positive T-cell lymphoma of childhood, EBV-positive CD8⁺ HLH					
Pt 4.1	Caucasian	4	Systemic EBV⁺ T-cell lymphoma of childhood	CD8⁺	Lymph node, CD8⁺
Pt 4.2	Caucasian	9	EBV⁺ CD8⁺ HLH during primary infection	CD8⁺	Bone marrow, CD8⁺
Pt 5.1	Caucasian	12	Hydroa vacciniforme	TCRγδ⁺	NP
Pt 5.2	Caucasian	5	Hydroa vacciniforme	TCRγδ⁺	NP
Pt 5.3	North African	40	Hydroa vacciniforme	TCRγδ⁺	NP
Pt 6.1	North African	3	Systemic T/NK cell CAEBV, mucocutaneous lymphoproliferation	CD8⁺, NK	Skin, CD8⁺
Pt 6.2	Turkish	15	Systemic T/NK cell CAEBV, recurrent HMG and fever	NK	Liver, CD3⁺
Pt 6.3	Sub-Saharan African	14	Systemic T/NK cell CAEBV, IBD	NK	Gut, CD3⁺
Pt 6.4	North African	7	Systemic T/NK cell CAEBV, mucocutaneous lymphoproliferation	CD4⁺; TCRγδ⁺	Lymph node, CD4⁺
Pt 6.5	North African	22	Systemic T/NK cell CAEBV, large-vessel vasculitis	TCRγδ⁺	NP
Pt 6.6	Sub-Saharan African	11	Systemic T/NK cell CAEBV, large-vessel vasculitis	CD3^low CD4⁻CD8⁻ TCRγδ⁻	NP
Pt 6.7	Pakistani	6	Persistent peripheral EBV load after rituximab, CD137/4-1BB deficiency (*TNFRSF9* hmz mutation: c.170delG/p.G57fsX91)	CD8⁺	NP
Pt 6.8	Caucasian	10	Systemic T/NK cell CAEBV, recurrent HMG and fever	CD8⁺	Liver, CD3⁺
Pt 6.9	Caucasian	35	Systemic T/NK cell CAEBV, indolent floor of the mouth tumor	CD4⁺	Floor of the mouth, CD4⁺
Pt S5	North African	52	Systemic T/NK cell CAEBV, chronic liver disease, SMG	CD4⁺; TCRγδ⁺	NP

Patients are numbered according to the figure number in which their PrimeFlow data are shown (first digit) and their place of appearance in the figure (second digit). GrB, granzyme B; hemiZ, hemizygous; HMG, hepatomegaly; hmz, homozygous; htz, heterozygous; IBD, inflammatory bowel disease; NP, not performed; PTCL-NOS, peripheral T cell lymphoma, not otherwise specified; SMG, splenomegaly.

involve non–B cell subsets. Samples from three pediatric patients referred to our laboratory with noncharacterized lymphoproliferations associated with persistent elevated blood EBV load (>5 log copies/ml) following hematopoietic stem cell (Pt 3.1), heart (Pt 3.2), or liver transplant (Pt 3.3) were first evaluated (Fig. 3 A). In two of them (Pt 3.1 and Pt 3.2), EBV load remained high after anti-CD20 treatment, indicating the persistence of EBV-infected cells that may not be B cells. In all three patients, EBER staining was found to be highly positive in a subset of CD3⁺ cells and to a lesser extent in the residual B cell compartment in two. In Pt 3.3, EBV infection of CD8⁺ T cells was confirmed by standard histologic staining showing CD3⁺EBER⁺ lymphocytes in the gut (Fig. 3 B). Thus, these findings indicate that lymphoproliferations in these patients can be considered as T cell PTLD.

Five adult patients with a histology-based diagnosis of NK or T cell lymphoma were next assessed. The first patient (Pt 3.4) presented with a symptomatic nasal form, and no circulating EBER⁺ cells were found in his PBMCs, in accordance with the negative result of blood EBV PCR. The four other patients had more misleading and diverse clinical presentations with elevated EBV load that required lymph node biopsies (Pt 3.5), recurrent skin biopsies (Pt 3.6 and Pt 3.8), a splenectomy (Pt 3.7), and a nasal biopsy in the absence of local symptoms (Pt 3.8) to complete the diagnosis (Table 1). In these latter patients, EBER staining revealed a positive subset among PBMCs likely corresponding to NK cells (CD3⁻CD2⁺CD56⁺ or CD3⁻CD2⁺CD16⁺), except for Pt 3.5, who was affected by CD3⁻CD4⁺ angioimmunoblastic lymphoma (Fig. 3 C). Arguing for an NK cell ontogeny of these EBER⁺ cells, CD16⁺ cells from Pt 3.8, which were almost all infected by EBV, were all strongly positive for the NK cell–specific markers CD160, DNAM1, NKp46, and 2B4, whereas CD3⁺ cells were negative (Fig. S3). Some of the EBER⁺ cells were also not stained by any extracellular marker (Pt 3.5, 3.7, and 3.8). They could represent malignant cells that have been shown to be positive for intracellular CD3 in ENKTL, which is not detected by our assay (Chan et al., 1996). Taken together, these results demonstrate that the PrimeFlow EBER assay enables a specific and sensitive detection and identification of EBV-infected circulating cells among PBMCs in various pathological conditions,
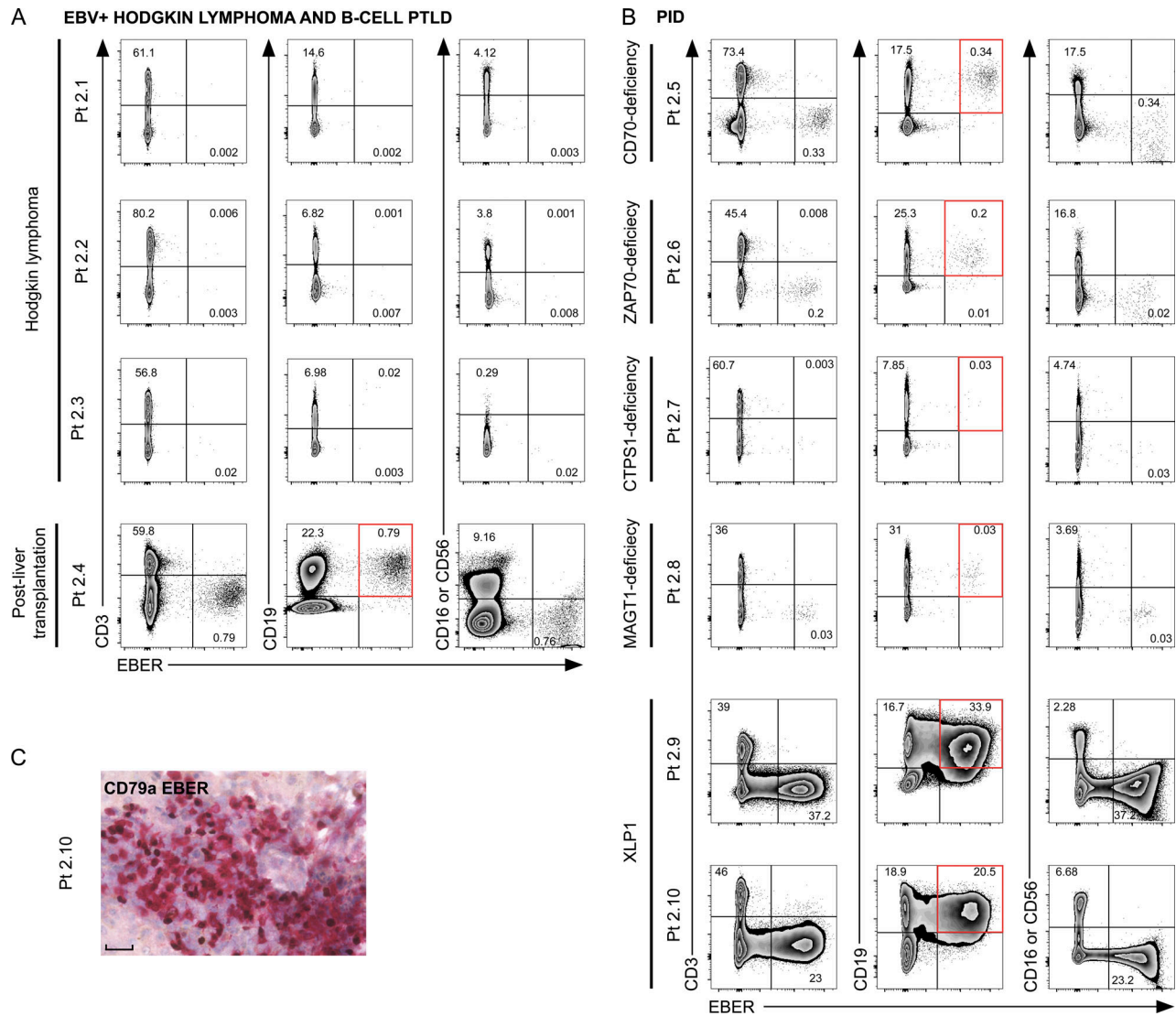
Fournier et al.
Detection of circulating EBV-infected cells

Journal of Experimental Medicine   6 of 20
https://doi.org/10.1084/jem.20192262

Figure 2. Detection by PrimeFlow EBER of peripheral EBV-infected B cells in PBMCs from patients with B-LPDs. (A and B) FACS dot plots of EBER expression by PrimeFlow assay coupled with anti-CD3, anti-CD19, anti-CD16, or anti-CD56 staining of PBMCs from patients affected with (A) Hodgkin lymphoma (Pt 2.1, Pt 2.2, and Pt 2.3) and post–liver transplantation B-LPD (Pt 2.4) or (B) B-LPD resulting from primary immune deficiencies, including CD70 (Pt 2.5), ZAP-70 (Pt 2.6), CTPS1 (Pt 2.7), and MAGT1 (Pt 2.8) deficiencies and XLP-1 (Pt 2.9, Pt 2.10). Dot plots are gated on eFluor⁻CD14⁻ cells. The red gates in the dot plots highlight the EBV-infected cell subsets. **(C)** Liver biopsy section from Pt 2.10 (XLP-1) that has been costained with an EBER probe and anti-CD79 antibody, showing infiltration of EBV-infected B cells. Magnification, ×400. Scale bar, 40 µm. Pt 2.10 analysis was repeated over time at different dates showing the same EBV-infected subset.

irrespective of the infected cell subsets. The presence of EBV-infected lymphocytes correlates in most of the patients with the clinical lymphoproliferation manifestations, EBV load, and histological findings. Therefore, this method provides a direct, rapid, and valuable diagnosis of EBV-driven B, T, and NK cell LPD.

Characterization of EBV-driven T/NK cell LPDs

Persistent infection of T and/or NK cells by EBV is underdiagnosed in Western countries, but it should be considered in patients with recurrent elevated EBV load, unusual clinical presentations of lymphoproliferation and HLH episodes, and/or no response to treatment with anti-CD20 antibodies. Moreover, this diagnosis is difficult to be rapidly obtained because it

depends on the accessibility of tissues for histological staining to detect EBV⁺ T and/or NK cells. Hence, the PrimeFlow EBER assay could represent a useful and potent tool to reach a rapid and earlier diagnosis without invasive procedures. Over the last years, we collected cases with noncharacterized lymphoproliferation and/or HLH manifestations associated with elevated and/or persistent blood/plasma EBV PCR over 6 mo and no biological or clinical response to B cell depletion after treatment with anti-CD20 (Table 1). 22 patients were recruited over a period of 5 yr, whose PBMCs were tested using the PrimeFlow EBER assay. On the basis of their clinical symptoms, patients can be classified into three groups according to Kim et al. (2019): (1) EBV⁺ CD8⁺ T cell HLH during primary infection (2 patients); (2) systemic EBV⁺ T cell lymphoma
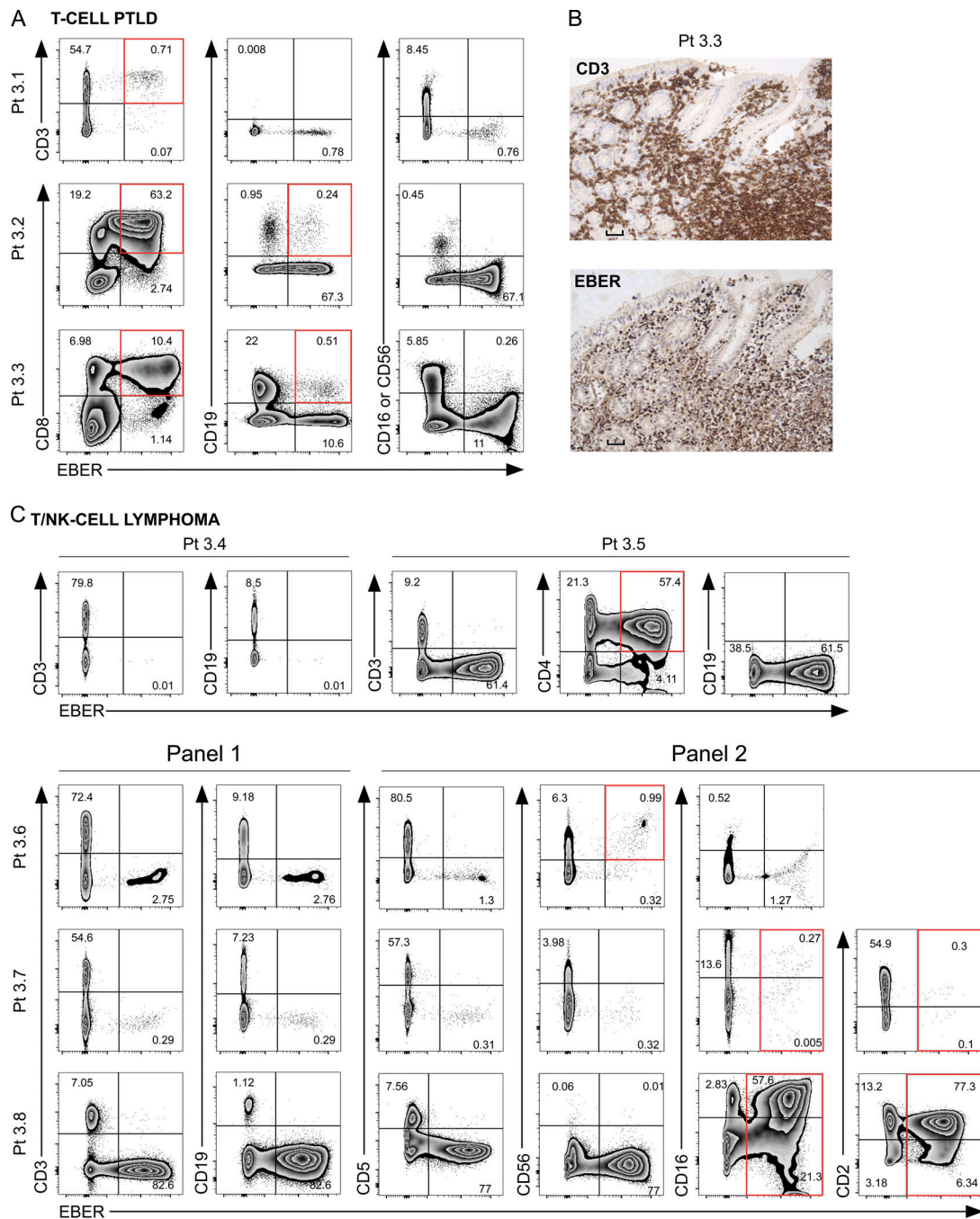
Figure 3. **PrimeFlow EBER detection of peripheral EBV-infected T and NK cells in patients with post-transplant EBV+ T/NK cell lymphoproliferation and ENKTL. (A)** FACS dot plots of EBER expression by PrimeFlow assay coupled with anti-CD3, anti-CD8, anti-CD16, anti-CD56, and anti-CD19 staining in PBMCs of patients with EBV+ T/NK cell lymphoproliferation after hematopoietic stem cell (Pt 3.1), cardiac (Pt 3.2), and liver transplant (Pt 3.3). A red square highlights the infected subset. Dot plots are gated on eFluor−CD14− cells. **(B)** Gut biopsy sections from Pt 3.3 stained with anti-CD3 or EBER probe showing infiltration of EBV-infected T cells. Magnification, ×200. Scale bars, 40 µm. **(C)** FACS dot plots of EBER expression using the PrimeFlow assay coupled with anti-CD3, anti-CD19, anti-CD4, anti-CD5, anti-CD56, anti-CD16, and anti-CD2 staining of PBMCs from patients with ENKTL. PBMCs used in panels 1 and 2 are from different time points, explaining the slight differences in proportions of EBER+ cells. Dot plots are gated on eFluor−CD14− cells. The red gates in the dot plots highlight the EBV-infected cell subsets. Pt 3.3, Pt 3.5, Pt 3.6, and Pt 3.7 analyses were repeated over time at different dates, showing the same EBV-infected subsets.

of childhood (1 patient); and (3) CAEBV of T and/or NK cell types (19 patients) that are further subdivided into cutaneous forms (hydroa vacciniforme–like LPD [3 patients] and mucocutaneous lymphoproliferation [2 patients]) and systemic forms (14 patients), with symptoms ranging from chronic and/or relapsing enlargement of lymphoid organs to various atypical autoinflammatory syndromes (e.g., inflammatory bowel disease [IBD], systemic vasculitis). Table 1 summarizes data only for the 14 patients for whom PrimeFlow EBER assay dot plots are shown.

Fournier et al.
Detection of circulating EBV-infected cells

Journal of Experimental Medicine   8 of 20
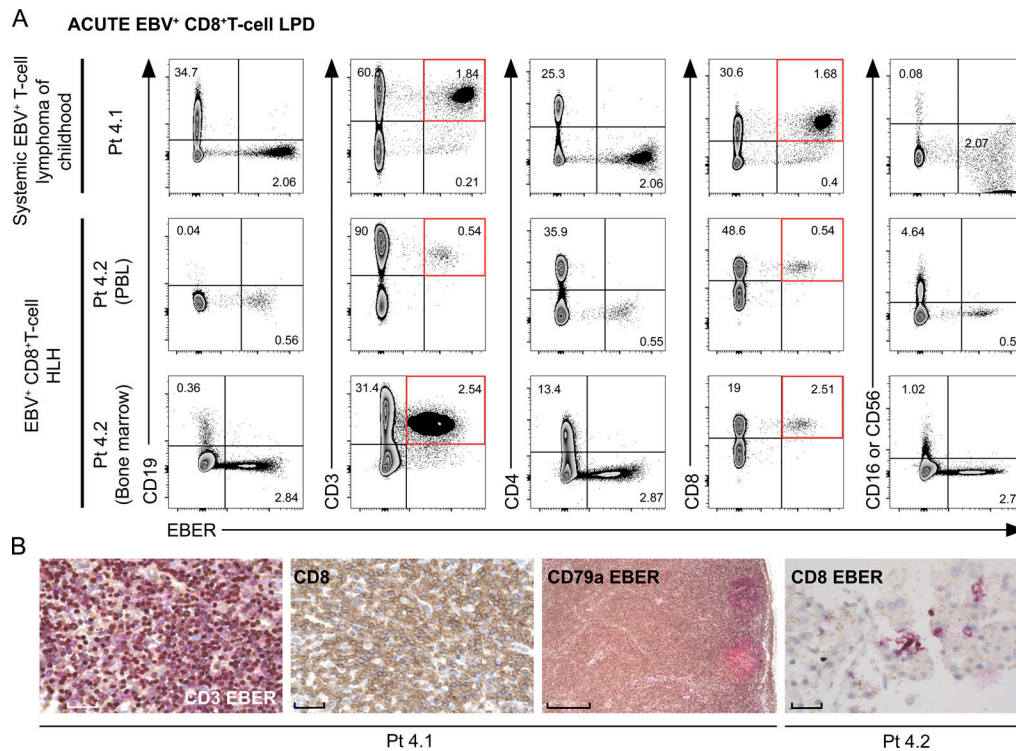https://doi.org/10.1084/jem.20192262

Figure 4. PrimeFlow EBER assay detects EBV-infected CD8⁺ T cells among PBMCs from patients with systemic EBV⁺ T cell lymphoma and EBV-associated HLH. (A) FACS dot plots of EBER expression by PrimeFlow assay coupled with anti-CD3, anti-CD4, anti-CD8, anti-CD16, anti-CD56, and anti-CD19 of PBMCs from patients with systemic EBV⁺ T cell lymphoma of childhood and EBV-associated HLH. Dot plots are gated on eFluor⁻CD14⁻ cells. The red gates in the dot plots highlight the EBV-infected cell subsets. **(B)** Lymph node biopsy section from Pt 4.1 costained with anti-CD3 and EBER probe (magnification, ×400) or stained with anti-CD8 (magnification, ×400) or anti-CD79a (magnification, ×50), showing infiltration by EBV-infected T cells. Liver biopsy section from Pt 4.2 costained with anti-CD8 and EBER probe showing infiltration of EBV-infected T cells (magnification, ×400). Scale bars, 40 μm, except for anti-CD79a, 200 μm.

Analysis of two patients meeting criteria of EBV⁺ T cell lymphoma of childhood (Pt 4.1) and severe EBV⁺CD8⁺ T cell lymphohistiocytosis (Pt 4.2) showed in both EBER⁺ cells restricted to CD8⁺ T cells in their PBMCs (1.84% and 0.54%, respectively) that were also detected in the material from bone marrow aspiration performed at the same time for Pt 4.2 (2.5% of total cells; Fig. 4 A). EBV-infected CD8⁺ T cells were observed by standard formalin-fixed, paraffin-embedded histology in
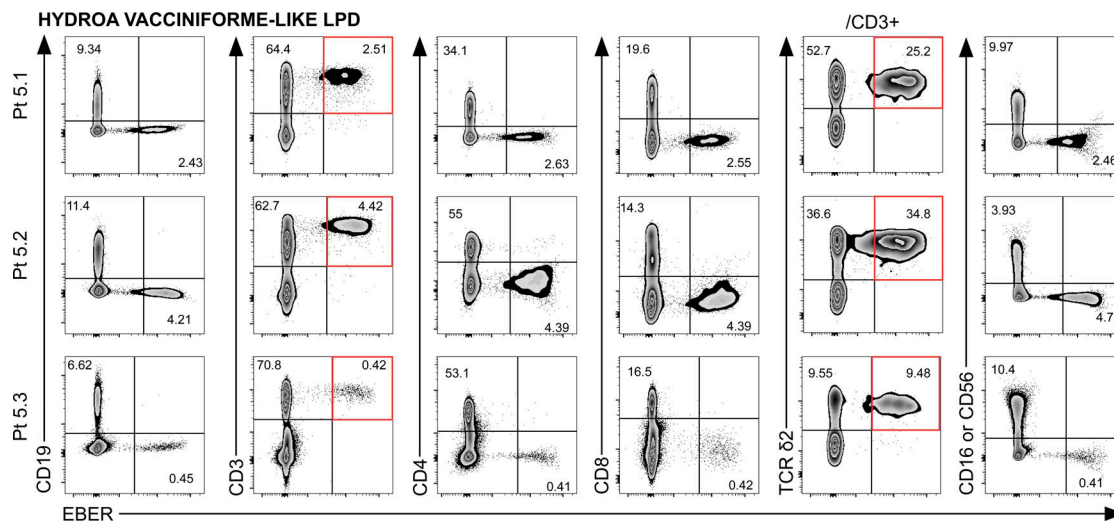

Figure 5. Patients with hydroa vacciniforme–like LPD showed circulating EBV-infected γδ2 T cells by PrimeFlow EBER assay. FACS dot plots of EBER expression by PrimeFlow assay coupled with anti-CD19, anti-CD3, anti-CD4, anti-CD8, anti-TCR δ2, anti-CD16, and anti-CD56 of PBMCs from Pt 5.1, Pt 5.2, and Pt 5.3 with hydroa vacciniforme–like LPD. The red gates in the dot plots highlight the EBV-infected cell subsets. All dot plots were gated on eFluor⁻CD14⁻ cells. Fraction of positive cells in the fifth column (/CD3⁺) is calculated as the percentage of total CD3⁺ T cells. Pt 5.1 analysis was repeated over time at different dates showing the same EBV-infected subset.

Fournier et al.
Detection of circulating EBV-infected cells

Journal of Experimental Medicine 9 of 20
https://doi.org/10.1084/jem.20192262

T- AND NK-CELL TYPE CAEBV, SYSTEMIC FORM

Figure 6. **Characterization of peripheral EBV-infected cells by the PrimeFlow EBER assay in patients suspected of systemic T/NK cell CAEBV.** FACS dot plots of EBER expression by PrimeFlow assay coupled with anti-CD19, anti-CD3, anti-CD4, anti-CD8, anti-CD16, and anti-CD56 of PBMCs from patients with systemic T/NK cell CAEBV. All dot plots are gated on eFluor−CD14− cells. The red gates in the dot plots highlight the EBV-infected cell subsets. PBMCs used for individual anti-CD16 and anti-CD56 staining (Pt 6.1, Pt 6.2, and Pt 6.3) are from different time points, explaining the slight differences in proportions of EBER+ cells. Pt 6.1, Pt 6.2, Pt 6.3, Pt 6.5, and Pt 6.8 analyses were repeated over time at different dates, showing the same EBV-infected subsets.

tissues (with EBER probe and anti-CD8 costaining) from both patients (Fig. 4 B). Regarding hydroa vacciniforme–like LPD, PBMC samples from three patients (Pt 5.1, 5.2, and 5.3) had an important proportion of EBV-infected γδ T cells, as previously described (Kimura et al., 2012). These T cells expressed the Vδ2 TCR chain (Fig. 5). Several patients with previously proven or suspected systemic forms of chronic active EBV infection of T/NK cell type with various clinical presentations were further

examined (Fig. 6). We also included analysis of an asymptomatic female carrier (Pt 6.7) of a *TNFRSF9* homozygous mutation previously reported in Rodriguez et al. (2019), who had a persistent high blood EBV load not relieved by anti-CD20 therapy. In all of these cases, the PrimeFlow EBER assay revealed either a single EBV-infected cell type or two EBV-infected cell types consisting of T and/or NK cells. Pt 6.3 also had circulating EBER+ B cells that may be related to the chronic immunosuppressive treatment he received. Importantly, these data correlated well with the infected subset(s) found by standard histology when available for Pt 6.1, 6.4, 6.8, and 6.9 (Fig. 6 and Fig. S3). Of note, histology revealed that two patients (Pt 6.2 and 6.3) had EBER+ CD3ε+ cells, whereas EBV-infected circulating cells corresponded only to NK cells that were repeatedly detected (Fig. S3, Table 1, and data not shown). This discrepancy is explained by intracellular expression of CD3ε of NK cells (Chan et al., 1996). Thus, the PrimeFlow EBER assay formally confirmed the diagnosis of CAEBV in these patients. Standard histology was not available for two patients (Pt 6.5 and 6.6) with systemic vasculitis who did not present any site to biopsy. In these cases, a systemic CAEBV diagnosis was only considered on the basis of results of the PrimeFlow EBER assay. Therefore, the PrimeFlow EBER assay appears to be an excellent and efficient tool to rapidly diagnose various EBV+ T/NK cell lymphoproliferations and to discriminate the infected cell subsets (as observed in these 22 cases). Hence, the assay can substitute for immunostaining of tissue biopsies, especially when no organ can be biopsied.

Correlation analyses between EBV load, EBV-infected cells, and clinical phenotypes

A potential relationship between whole-blood EBV load and the percentage of circulating EBER+ cells detected by the PrimeFlow EBER assay was examined. Individuals with B-LPD or T/NK-LPD tested with the PrimeFlow EBER assay were analyzed, including all patients listed in Table 1, in addition to seven other patients with NK/T-LPD and nine other patients with B-LPD. A significant positive correlation was found starting from EBV loads above 4 log copies/ml, whereas the number of EBER+ cells was not significantly different from the false-positive background in most cases with EBV loads below 4 log copies/ml (Fig. 7 A). The percentage of infected cells among each cell subset was also evaluated according to the disease classification (Fig. 7 B). The proportion of circulating EBV-infected B cells was below 10% in patients with B cell lymphoproliferation, with the exception of the two patients with XLP-1 who had EBV+ B cell lymphocytosis and one patient (Pt S4) shown in Fig. S4 (>40% of infected B cells).

Both patients with systemic EBV+ T cell lymphoma of childhood and EBV+ T cell HLH had a low proportion of circulating EBER+ CD8+ T cells (ranging from 1.1% to 10%; Fig. 7 B). In contrast, in patients who presented with systemic T/NK-LPD/ CAEBV, the proportion of infected cells was found to be much higher, as exemplified by patients with hydroa vacciniforme–like LPD, who all exhibited a high proportion of EBV-infected TCR Vδ2 T cells, ranging from 14.5% to 60%. In other patients with systemic CAEBV, distinct T cell subpopulations were found to be infected, including CD4, CD8, and NK cells. Three patients

had two infected subsets (CD4+ and NK cells [n = 1] and CD4+ and TCR γδ+ [n = 2]). Thus, with the exception of patients with hydroa vacciniforme–like LPD, HLH, and systemic lymphoma of childhood, no clear association could be made between the clinical phenotypes and the nature of the infected cell subsets.

Advantage of PrimeFlow EBER assay over EBV PCR on sorted cells

Discrimination of EBV-infected cells among PBMCs can be performed by a specific PCR for EBV on sorted cells. However, the cell-sorted fraction may be falsely positive because of the purity of sorted cells, which is never 100%, and residual cell-free EBV DNA that may still be present. An example of such a false-positive result is depicted in Fig. S4. EBV loads only slightly decreased in a 5-yr-old patient with severe symptoms of IM suggestive of a primary infection (with anti-viral capsid antigen [VCA] IgM+, anti-VCA IgG−, and anti-EBNA IgG−) despite effective B cell depletion after three injections of anti-CD20 (Pt S4 in Table 1). PCR for EBV on sorted cells was then performed and revealed 3.5 log copies/10^5 cells and 4.9 log copies/10^5 cells of EBV in CD3+ and CD3− cells, respectively. Because no B cell had been detected before sorting, no contamination of the CD3+ fraction was expected, and no purity check was therefore performed after sorting. The PrimeFlow EBER assay performed in parallel showed EBER staining only in a subset expressing low amounts of CD19, whereas neither T nor NK cells were positive (Fig. S4 B). Additional courses of anti-CD20 treatment eventually significantly reduced the EBV load (Fig. S4 A), and only EBV+ B cells without EBV+ T or NK cells were detected in a lymph node biopsy detected by immunostaining (Fig. S4 C). Thus, the PrimeFlow EBER assay appears to be more reliable at discriminating EBV-infected cells than the detection of EBV by PCR on sorted cells.

Phenotypic characterization of EBV-infected B and T cells

We evaluated whether the PrimeFlow EBER assay could be suitable for further characterization of EBV-infected cells. One strength of the PrimeFlow assay is the large panel of extracellular antibodies that can be used (Table S1). The precise phenotypes of EBV-infected cells in EBV-related disorders are not well known. Thus, EBV-infected B cells and T cells were characterized in more detail in several patients. We first examined EBER+ B cells of one XLP-1 patient (Pt 2.10; shown in Fig. 2 B) during a fulminant IM course (Fig. 8 A). These cells divided into two subsets based on CD19, CD21, CD27, CD38, and IRF4 expression. One was CD19highCD21highCD27lowCD38intIRF4low, and the second was CD19lowCD21lowCD27highCD38highIRF4int/high, evoking germinal center B cells and plasma cells, respectively (Kassambara et al., 2015). In contrast to the intracellular staining for IRF4, the PrimeFlow EBER assay did not work with intracellular BCL6 staining using our available antibody (data not shown). However, all CD19low cells and a large proportion of CD19high cells were stained for BCL6, suggesting that the majority of EBER+ B cells expressed BCL6. Both subsets were IgM+, IgDlow/−, and CD80+. We next analyzed EBER+ T cells from two patients with CAEBV (Pt 6.8 and Pt 6.9; shown in Fig. 6). A homogeneous effector memory CD27−CD45RA− phenotype with
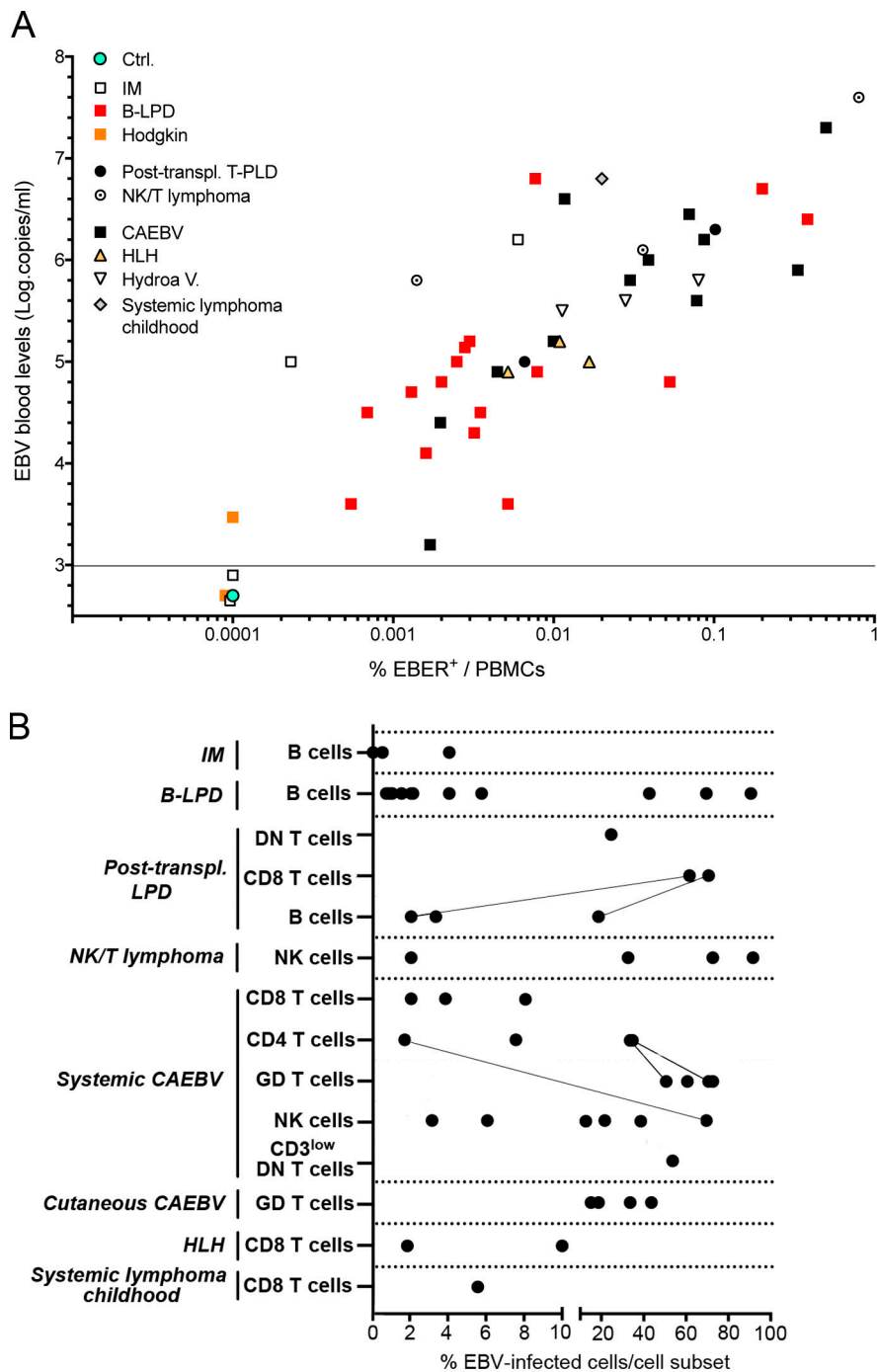
Fournier et al.
Detection of circulating EBV-infected cells

Journal of Experimental Medicine
https://doi.org/10.1084/jem.20192262

11 of 20

Figure 7. **Relationships between EBV-infected cell fraction, EBV load, and clinical phenotypes. (A)** Percentage of EBV-infected cells among PBMCs plotted against EBV loads detected from whole blood by PCR (log copies/ml), including both healthy control and patient samples. Control corresponds to distinct data of 13 different healthy donors with EBV load below log 2.7, which is the limit of detection. 0.001% of EBER$^+$ cells is considered the limit of detection of EBER$^+$ cells. **(B)** Percentages of EBV-infected cells among the infected cell subsets from PrimeFlow EBER analysis of B cells correspond to CD3$^-$CD19$^+$ cells, CD4 T cells correspond to CD3$^+$CD4$^+$CD8$^-$, CD8 T cells correspond to CD3$^+$CD4$^-$CD8$^+$, double-negative (DN) T cells correspond to CD3$^+$CD4$^-$CD8$^-$, CD3^{low} DN T cells correspond to CD3^{low}CD4$^-$CD8$^-$, GD T cells correspond to CD3$^+$ γδ TCR, and NK cells correspond to CD3$^-$CD16$^+$ and/or CD56$^+$. Line-connected dots represent two infected subsets in a single patient. All data from dot plots in A and B are gated on eFluor$^-$CD14$^-$ cells. Data from patients listed in Table 1 are depicted, supplemented with data from additional patients with B-LPD (n = 9) and T/NK CAEBV (n = 7).

an increased expression of the HLA-DR activation marker was observed in both (Fig. 8 B). In contrast, EBER$^-$ T cells were heterogeneous, comprising naive, effector, and, memory cell subsets. These data suggest that EBV triggers both T and B cells to differentiate into activated effector memory T cells and plasma cells, respectively.

To gain more insight into the type of latency that is associated with EBV-infected T cells, we used the PrimeFlow assay to detect concomitant expression of transcripts for LMP1 or EBNA2 using specific probes (coupled to a fluorochrome different from the one of the EBER probe). Although we were able to detect EBNA2 transcript expression and heterogeneous LMP1 transcript expression in LCL cells, we failed to detect EBNA2 or LMP1 expression among EBER$^+$ cells of four CAEBV patients (Pt 3.3, 5.1, 6.4, and 6.8). However, we found a low proportion of cells expressing EBNA2$^+$ transcripts among EBER$^+$ B cells from an XLP1 patient (Pt 2.9), but no expression of LMP1 transcripts (Fig. S5 A).

The mechanisms of infection of T and/or NK cells by EBV remain elusive. One hypothesis is that it is mediated by trogocytosis, a phenomenon whereby exchange of cellular material occurs at the immune synapse (Joly and Hudrisier, 2003). EBV
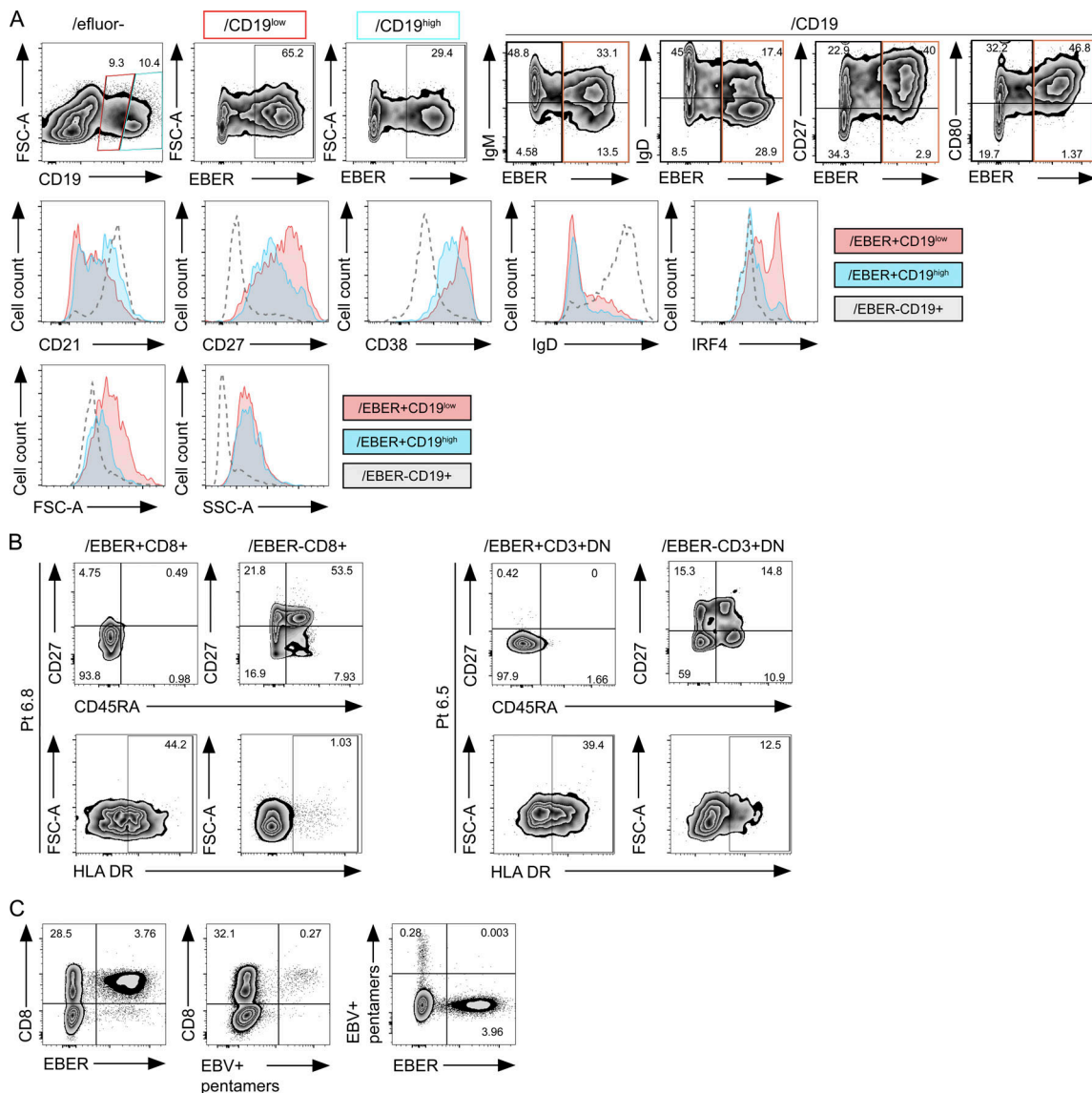
Fournier et al.
Detection of circulating EBV-infected cells

Journal of Experimental Medicine   12 of 20
https://doi.org/10.1084/jem.20192262

Figure 8. **Phenotypes of EBV-infected B and T cells. (A)** FACS dot plots and histograms of EBV-infected CD19⁺ cells using the PrimeFlow EBER assay coupled with anti-IgM, anti-IgD, anti-CD27, anti-CD80, anti-CD21, anti-CD27, anti-CD38, and anti-IRF4 staining in addition to size (forward scatter [FCS]) and granularity (side scatter [SSC]) from PBMCs of a patient with XLP-1 during fulminant IM (Pt 2.10). Upper panels, cells gated on CD19^{low} (/CD19^{low}), CD19^{high} (/CD19^{high}), or CD19 (/CD19). Middle and lower panels, cells gated on EBER⁺CD19^{low} (/EBER⁺CD19^{low}), EBER⁺CD19^{high} (/EBER⁺CD19^{high}), or EBER⁻CD19⁺ (/EBER⁻CD19⁺). **(B)** FACS dot plots using the PrimeFlow EBER assay coupled with anti-CD3, anti-CD4, anti-CD8, anti-CD27, anti-CD45RA, and anti-HLA-DR staining from PBMCs of two patients, one with CAEBV associated with EBV-infected CD8⁺ T cells (Pt 6.8) and one with EBV-infected γδ T cells (Pt 6.5). Dot plots from gating on EBER⁺CD8⁺ (/EBER⁺CD8⁺) or EBER⁺CD3⁺CD4⁻CD8⁻ (/EBER⁺CD3⁺DN). **(C)** FACS dot plots using the PrimeFlow EBER assay coupled with anti-CD3, anti-CD8, and EBV-specific HLA-A2* pentamer staining showing EBV-specific T cells from PBMCs of Pt 6.8. All dot plots are gated on eFluor⁻CD14⁻ cells.

may be transmitted to T or NK cells through a synapse between infected B cells and EBV-specific cytotoxic T or NK cells, either directly or through membrane exchange including CD21, the receptor for EBV expressed on B cells (but not on T or NK cells; Tabiasco et al., 2003; Lee et al., 2018). If this assumption was correct, EBV-infected T cells should be specific for EBV peptides presented by infected B cells. This was tested in a patient (Pt 6.8) presenting with a high proportion of blood EBV-infected CD8 T cells and expressing HLA-A2 molecules, for which tetramers specific for EBV-derived peptides are available (Fig. 6). 0.8% of CD8⁺ T cells were recognized by the HLA-A2-EBV pentamer

(0.21% of total cells). However, EBER⁺ T cells were not stained with the HLA-A2-EBV pentamer (Fig. 8 C). These findings suggest that trogocytosis is not a major mechanism accounting for the entry of EBV into T cells, at least in the patient tested here.

We next analyzed whether the presence of EBV in T cells could influence CD8⁺ or CD4⁺ T cell functions from PBMCs of Pt 6.8 and Pt 6.9, who harbored CD8⁺ and CD4⁺ EBV-infected T cell subsets, respectively (Fig. 9). CD3-induced T cell proliferation and degranulation assays were performed and compared between infected and noninfected cells that were discriminated with the PrimeFlow EBER assay. Because these functional assays
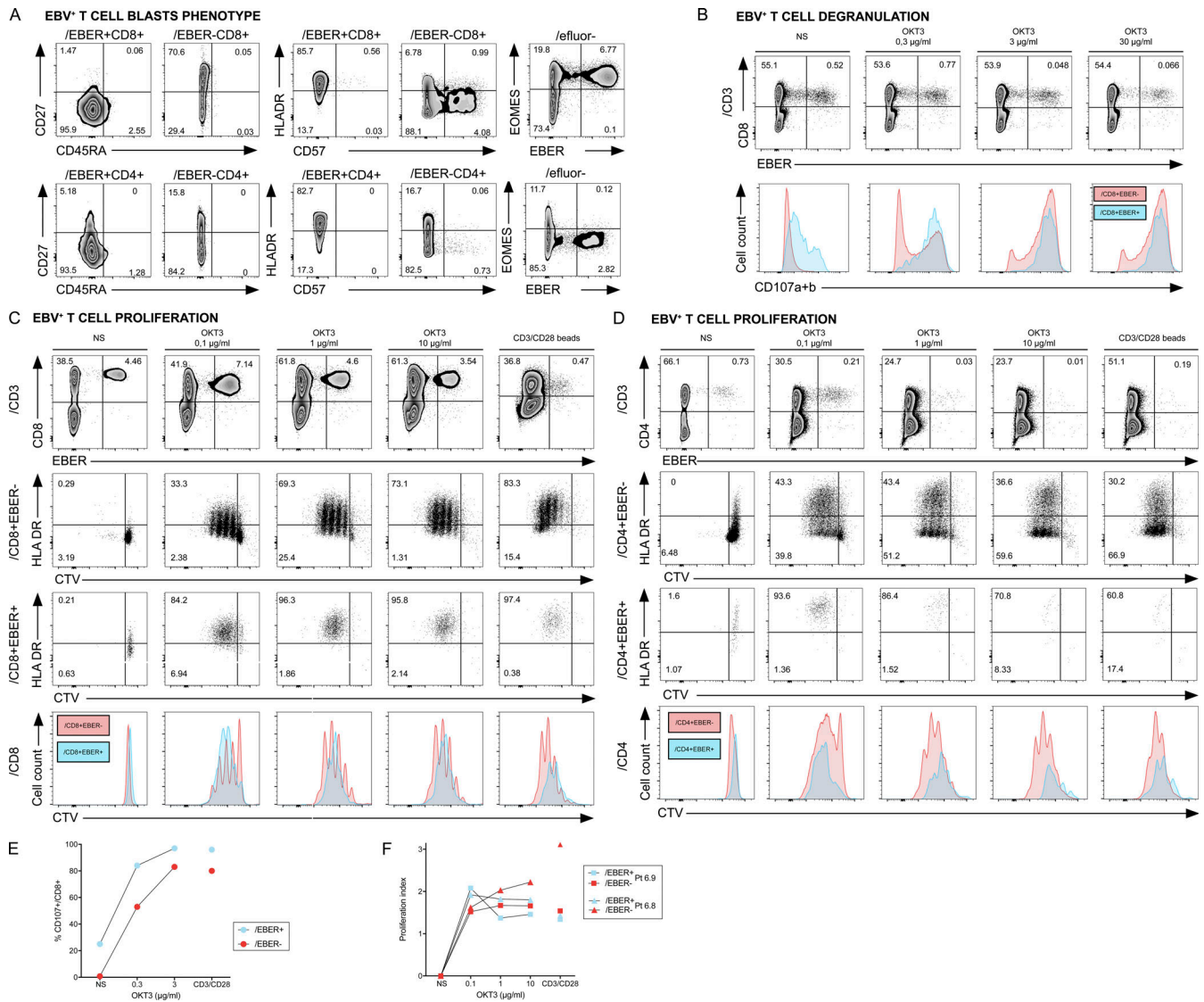
Figure 9. **Functional characterization of EBV-infected T cells. (A)** FACS dot plots using PrimeFlow EBER assay coupled with extracellular staining for CD3, CD4, CD8, CD27, CD45RA, and HLA-DR or with intranuclear staining for EOMES from T cell blasts of two patients affected with CAEBV associated with EBV-infected CD8+ T cells (Pt 6.8) or EBV-infected CD4+ T cells (Pt 6.9). Dot plots from gating on EBER+CD8+ (/EBER+CD8+), EBER+CD3+CD4+ (/EBER+CD4+), or eFluor− cells (/eFluor−). **(B)** FACS dot plots (upper panels) and histograms (lower panels) of anti-CD3 (OKT3)–induced degranulation assay of T cell blasts from Pt 6.8 assessed by staining for CD8 and CD107a/b surface, followed by the PrimeFlow EBER assay. FACS dot plots showing EBV-infected (EBER+CD8+) or noninfected (EBER−CD8+) T cells and overlaid histograms showing CD107a/b expression in gated EBER+CD8+ (blue) or EBER−CD8+ (red) cells for each stimulation condition. Concentrations in µg/ml of OKT3 are indicated along with nonstimulated cells (NS). **(C and D)** FACS dot plots (upper panels) and histograms (lower panels) of anti-CD3 (OKT3)–induced proliferation of T cell blasts from Pt 6.8 (C) and Pt 6.9 (D) assessed with staining with CellTrace Violet (CTV) dye, followed by PrimeFlow EBER coupled with staining for CD4 (D), CD8 (C), and HLA-DR. FACS dot plots showing EBV-infected (EBER+) or noninfected (EBER−) T cells (upper panels), CTV, and HLA-DR expression in gated CD8+EBER+ or CD8+EBER− cells (C, middle panels) and CD4+EBER+ or CD4+EBER− cells (D, middle panels) and overlaid histograms showing CTV expression in gated EBER+ (blue) or EBER− (red) cells for each stimulation condition. Concentrations in µg/ml of OKT3 are indicated along with nonstimulated (NS) cells. All dot plots are gated on eFluor−CD14− in A–D. **(E)** Graphed data of the percentage of degranulation (CD107+ cells among CD8+) from the amounts shown in B. **(F)** Index of proliferation calculated from the experiments showed in C and D.

require important numbers of cells to be analyzed, they were conducted on expanded T cell blasts from PBMCs. Phenotyping of T cell blasts in both patients revealed that most EBV+ T cells had an effector memory phenotype (CD27−CD45RA−), were activated (HLA-DR+), and were not senescent (CD57−). By contrast, EBV− cells had rather an effector or central memory phenotype (CD27+CD45RA−), were not activated, and a small proportion was senescent (Fig. 9 A). Notably, all EBV+CD8+ T cells (in Pt 6.8)

were found to express the transcription factor EOMES, well known to be associated with peripheral CD8+ T cell differentiation. The proportion of EBV+ T cells was stable in culture; thus, EBV+ cells did not seem to have a selective advantage in the conditions of culture used. Interestingly, EBV+CD8+ T cells already expressed significant amounts of the degranulation markers CD107a/b without any stimulation, in contrast to noninfected CD8+ T cells (Fig. 9, B and E). Under stimulation

with a low dose of anti-CD3, CD107a/b expression was strongly increased on the vast majority of EBV$^+$ CD8$^+$ T cells. This may point to a particular role of EBV in activation of infected T cells. Proliferation of EBV$^+$CD8$^+$ and CD4$^+$ T cells was also increased at low doses of anti-CD3, whereas it was decreased at higher doses and in response to CD3/CD28 stimulation (Fig. 9, C, D, and F). This decrease correlated with a strong reduction of the proportion of EBV$^+$ T cells, which may at first sight indicate a loss by activation-induced cell death (AICD). However, we did not find any evidence of increased AICD of these cells (data not shown). Because AICD was apparently not increased in infected cells, it may suggest a potential downregulation or decay of EBERs. Additional experiments are warranted to test this hypothesis. Thus, these findings suggest that EBV modulates terminal differentiation and threshold of TCR activation in CD4$^+$ and CD8$^+$ infected cells. Finally, we investigated cytokine production by intracellular staining for IFN-γ, TNF-α, and IL-2. In PBMCs from four EBV$^+$ T/NK-LPD patients (Pt 3.3, 5.1, 6.4, and 6.8), no cytokine production was detected (Fig. S5 B). However, a slight increase in the proportion of stimulated T cell blasts from Pt S5, but with a lower MFI (indicating probably a lower amount per cell), was detected (Fig. S5, C and D). Taken together, these observations show that functional studies on either infected or noninfected cells can be performed at the same time using the PrimeFlow EBER assay.

Discussion

In this study, we describe the PrimeFlow RNA assay, which allows both rapid and reliable detection and characterization of EBV-infected cells from fluid samples, including blood and bone marrow. The assay uses conventional flow cytometry with antibody-based staining of membrane extracellular markers in combination with a specific DNA probe for EBERs, thus enabling the discrimination of the EBV-infected cell subset(s) (Henning et al., 2016). This method has been previously used in a humanized mouse model of EBV infection (McHugh et al., 2017). Because EBERs are abundantly expressed in all infected cells, regardless of the type of latency involved (Lerner et al., 1981), they represent the best markers for detection of EBV presence within cells. Some laboratories have used EBV-specific PCR on sorted cells to detect and characterize circulating EBV-infected cells as an alternative to conventional histology (Zhang et al., 2019), but this approach is cumbersome and may lead to false-positive findings through contamination of the T or NK cell or non–B cell fraction by either infected B cells or plasma EBV DNA, as shown herein in Fig. S4.

The PrimeFlow EBER assay revealed good reproducibility, showing the same EBV-infected cell populations when performed on several occasions in the same patients (Pt 2.10, 3.3, 3.5, 3.6, 3.7, 5.1, 6.1, 6.2, 6.3, 6.5, and 6.8; see figure legends), and was found to be concordant with immunohistochemistry and coimmunostaining data when available. In most of the patients, circulating EBV-infected lymphocyte subsets (identified by PrimeFlow) corresponded to the same infected cell populations detected in tissue biopsies by immunostaining. Flow-FISH assays using probes for EBERs have been developed previously (Kimura et al., 2009; Kawabe et al., 2012); however, they worked only with a restricted panel of extracellular antibodies for which buffers and reagents were not specifically developed to sustain proper extracellular staining (Kimura et al., 2009). Moreover, signal amplification of the EBER probe in these assays was low. These technical limitations may impair diagnosis, especially for patients with a very low number of circulating infected cells. None of these tests are available for routine laboratory diagnostics. By contrast, the PrimeFlow FISH assay reported here was able to preserve cell surface and intracellular staining with a wide range of antibodies and to sustain a high EBER signal, allowing us to easily discriminate infected cells. Moreover, in our assay, we use a viability dye, which further improves the gating on living cells and decreases the risk of false-positive or false-negative staining. The previous studies used forward and side scatter profiles, which are strongly altered after fixation and permeabilization.

We failed to detect infected cells in PBMCs of healthy donors seropositive for EBV. Circulating EBV-infected memory B cells that represent the EBV reservoir are considered to be very scarce, below 1 in 100,000 total circulating B lymphocytes (Laichalk et al., 2002). This is very likely under the threshold of detection of our method. No or rare circulating infected cells were noticed in patients with EBV-related Hodgkin lymphoma, although EBV was detected in the serum or whole blood by PCR. This is not surprising, because Hodgkin lymphoma cells are restricted to lymphoid tissues with no or few circulating cells, and detection of EBV in blood by PCR relies much more on EBV plasma content than on mononuclear cells in this context (Hohaus et al., 2011). The positive blood EBV load in patients with Hodgkin lymphoma is likely explained by EBV released in the plasma from apoptotic neoplastic cells from tissues (Ryan et al., 2004; Kimura and Kwong, 2019). Hence, because our method cannot detect tissue-resident EBV-infected cells, it is not suitable for pathologies in which EBV-infected cells are not circulating in the blood.

In individuals with IM, circulating EBV-infected cells were detectable only in the most severe forms with elevated EBV loads. Thus, we inferred that the PrimeFlow EBER assay is powerful enough to detect infected cells during ongoing infection but not for convalescent or asymptomatic carriers. The low proportion of infected B cells detected in the periphery is within the same range as in previous studies that used PCR for EBV with limited cell dilution conditions in individuals with IM and patients with solid organ transplantation (Babcock et al., 1999; Hochberg et al., 2004). Overall, our data show a positive correlation between the proportion of circulating EBV-infected cells and EBV loads, but they reveal limitations regarding sensitivity: In patients with low EBV loads (below 4 log copies/ml of EBV), detection of EBV-infected cells is ineffective and thus noninformative.

In patients in whom very few circulating infected cells are detected, results need to be interpreted with caution, and careful interpretation of positive cells is required to confirm the diagnosis. Acquisition of a higher number of cells (>3 million) can help to highlight one or two small clusters of cells with high MFI corresponding to EBV-infected cells. Inclusion of control probes

is necessary and contributes to an accurate diagnosis in this situation. Importantly, staining with the Bacillus probe helps to exclude false-positive EBER+ cells related to autofluorescence or rare events of nonspecific hybridization (see Fig. S2). Indeed, in contrast to truly EBER+ cells, the Bacillus-staining MFI is lower and heterogeneous, generating a smear shape rather than a homogeneous cluster. When cellular material is scarce with poor viability (possibly due to the poor clinical condition of the patient), it is advisable to include both a viability dye and the positive control probe (targeting the ubiquitous RPL13A ribosomal RNA) to secure both procedure and diagnosis.

Based on the most recent diagnosis criteria from the World Health Organization classification of tumors of hematopoietic and lymphoid tissues (Swerdlow et al., 2016) and the Committee on Measures against Intractable Diseases of the Ministry of Health, Labour and Welfare of Japan (Arai, 2019), demonstration of EBV-infected T or NK cells is required to establish the diagnosis of T/NK CAEBV or EBV+ T/NK LPD. This diagnosis is usually achieved by immunostaining of tissue biopsies. However, clinical conditions for organ biopsies are not always fulfilled, especially when facing organ failure associated with severe HLH. Importantly, our study shows that all patients with histologically proven CAEBV had detectable blood EBV-infected T or NK cells, which are easier to access. In addition, the PrimeFlow EBER assay enables correct diagnosis of patients without an identified lesion to biopsy, as illustrated by two patients with atypical systemic vasculitis (Pt 6.5 and Pt 6.6). Similarly, circulating EBV+ NK-like cells were detected by the PrimeFlow EBER assay in two patients (Pt 3.5 and Pt 3.7) before diagnosis of ENKTL by histology. This was rather an unexpected finding because positive EBV load in these patients is thought to be due to release of EBV DNA from in situ tumoral cells (Kimura and Kwong, 2019). Importantly, this may indicate a transition from a latent form of CAEBV to overt lymphoma. Hence, the PrimeFlow EBER assay has three important advantages: (1) It avoids harmful invasive procedures in patients with a poor clinical condition; (2) it permits a diagnosis in the absence of access to pathological tissue; and (3) it leads to an early and rapid diagnosis and thus to adapted therapies and can be used as a biomarker of treatment efficacy. Furthermore, the mere detection of infected cells in some diseases could give insight into their progression and their pathophysiology.

EBV+ T/NK-LPD, including T/NK CAEBV diseases, is mostly prevalent in native Asian and American populations. In Western countries, EBV+ T/NK-LPD diagnosis is often not considered or considered last. Nevertheless, we recruited more than 20 patients of Caucasian or African origin with atypical (e.g., vasculitis, autoimmunity) or typical (HLH, hydroa vacciniforme) clinical presentations of T/NK-LPD associated with a high blood EBV load, poor response to anti-CD20 treatment, and/or persistent EBV load. Thus, our observations stress that patients with T/NK-LPD are not as geographically and ethnically restricted as reported previously. On the whole, our patients showed infected-cell subsets quite similar to those of Asian/Japanese patients previously analyzed (Kimura et al., 2012).

We did not observe any correlation between clinical presentation and the type of EBV-infected subsets, with the exception of patients with hydroa vacciniforme–like LPD and HLH, who exhibited EBV-infected γδ T cells and CD8+ T cells, respectively. The presence of EBV-infected γδ T cells has previously been associated with hydroa vacciniforme–like LPD (Kimura et al., 2012). Here, the three patients with hydroa vacciniforme exhibited circulating EBV-infected TCR Vδ2 T cells. The reason for this selective expansion of EBV+ TCR Vδ2 T cells remains undetermined. As previously reported (Kimura et al., 2012), circulating EBV-infected CD8+ T cells were detected only at a low proportion in two patients, one with EBV+ T/NK-LPD–related fulminant HLH (Pt 4.1) and one with EBV+ CD8 T cell lymphoma of childhood (Pt 4.2), although they had a significant EBV load (>4 log copies/ml). Likely, the low proportion of circulating EBV+ cells does not reflect the level of infected cells in tissues. In fact, a higher proportion of infected CD8+ T cells was found in the bone marrow sample of Pt 4.2 by the PrimeFlow assay, and an important EBV+ CD8 T cell infiltration was shown by histology in Pt 4.1.

The conserved extracellular, intracytoplasmic, or intranuclear staining may be especially relevant regarding the study of the pathophysiology of EBV-related disorders. Notably, we show that this assay can be used to directly assess properties and characteristics of infected cells in a more physiological setting without the need of cell sorting. In particular, it allows detailed phenotyping of EBV-infected B, T, or NK cells and functional studies. This is first illustrated by the XLP-1 case with a fulminant IM course (Pt 2.10), in whom we found that EBV-infected B cells harbored germinal center and plasmablast markers. Interestingly, these findings may support the germinal center hypothesis stating that EBV-infected naive B cells are driven to germinal center cell differentiation (Thorley-Lawson and Babcock, 1999; Thorley-Lawson et al., 2013). However, XLP-1 patients have an impaired capacity to form germinal centers and to undergo immunoglobulin class switching (Ma et al., 2006), indicating that EBV could also directly provide signals that mimic germinal center differentiation without requiring T cell help and/or germinal center transit, although those would not be sufficient for class switching, because EBER+ B cells are only IgM+. These data are concordant with the previous study of Chaganti et al. (2008) showing that EBV+ infected B cells which persist in XLP-1 patients after IM are CD27+IgM+.

Regarding T/NK-LPD, we showed that EBV-infected CD8 and γδ T cells (in Pt 6.8 and 6.5, respectively) had an effector memory cell phenotype in contrast to noninfected cells. EBV-infected T cell blasts from patients also had an effector memory cell phenotype with strong activation markers, including increased degranulation capacity and no expression of the senescent CD57 marker despite a strong expression EOMES (known to be associated with T cell exhaustion and senescence). Consequently, EBV may be directly involved in activating or lowering the threshold of activation in CD4+ and CD8+ infected cells. Although we failed to detect increased IFN-γ content or production in EBV+ T cells in the five tested patients, it will be of interest to determine if increased IFN-γ production by EBV+ T cells could correlate with the appearance of HLH symptoms, which are known to be driven by excessive IFN-γ production by T cells.

Fournier et al.
Detection of circulating EBV-infected cells

Journal of Experimental Medicine   16 of 20
https://doi.org/10.1084/jem.20192262

LMP1 and/or LMP2 have previously been shown to interfere with TCR signaling and functions of Jurkat cells (Ito et al., 2014; Ingham et al., 2005). We did not detect LMP1 transcripts in EBER+ T cells from four patients tested or in EBER+ B cells of one XLP-1 patient (whereas EBNA2 transcripts were detected in few EBER+ B cells; see Fig. S5). This finding may be explained by a weak sensitivity of the probe and/or the low level of LMP1 transcripts (compared with EBER) in EBV-infected T cells, as previously noticed by Iwata et al. (Iwata et al., 2010). LMP1 and EBNA2 transcripts in EBV-infected B cells were found to be weakly expressed at levels similar to those of EBER transcripts (Tierney et al., 2015). Additional studies will be necessary to characterize the molecular mechanisms through which EBV impedes T cell responses.

We have found no evidence that EBV-infected CD8+ T cells were specific for EBV (in one patient tested) by coupling the PrimeFlow EBER assay to EBV-HLA-A2 pentamer staining. However, this does not formally exclude a role for trogocytosis, because EBV+ T cells may recognize other EBV peptides not contained in the HLA-A2 pentamer used here. Further assessments with other peptides and more patients are warranted. Alternatively, other mechanisms of T or NK cell infection may occur, such as infection of early T cell precursors that have been shown to express CD21 (Pekalski et al., 2017).

In conclusion, we describe a novel flow-FISH method allowing easy and rapid detection of EBV-infected cells in blood and bone marrow samples. We show that this assay represents a reliable tool to diagnose EBV+ T/NK-LPD, a rare and severe group of diseases. Implementation of this assay as a routine screening test in clinics should make diagnosis easier, thereby increasing the identification of patients presenting with these disorders, which are most likely underdiagnosed, especially in Western countries. This could be included in the diagnostic algorithm for T/NK-LPD recently proposed by Hue et al. (2020). This should also help clinicians to monitor the response to treatments and lead to patient-tailored precision medicine (e.g., through further molecular description of these EBV-infected cells), such as by the analysis of markers such as PD-1 and CD30, for which targeting antibodies have been proved to be effective (Hu and Oki, 2018). Finally, this assay opens new perspectives to study EBV-infected cells using single-cell transcriptomic and genomic approaches and thus will contribute to a better understanding of the physiopathological mechanisms of EBV-driven LPD.

Materials and methods
Ethics
Written informed consent was obtained from all human participants in this study in accordance with the Helsinki declaration, local legislation, and ethical guidelines from the Comité de Protection des Personnes de l'Ile de France II, Hôpital Necker-Enfants Malades, Paris. Blood from healthy donors was obtained at the Etablissement Français du Sang organization under approved protocols (convention 15/EFS/012).

EBV DNA blood load quantification
EBV DNA quantification was performed with the EBV R-GENE assay from Argene according to the manufacturer's recommendations. This commercial kit is based on a real-time PCR technique amplifying a fragment of the viral thymidine kinase gene (BXLF1) with a threshold value of four genome copies per PCR well. The lower limit of detection is set at 2.7 log copies/ml. Log 2.7 is considered as negative. Data were obtained from routine laboratory tests.

Cell culture and stimulation
PBMCs were isolated by Ficoll-Paque (Lymphoprep; ProteoGenix) density-gradient centrifugation, washed, and resuspended at a density of 10^6 cells per ml in complete Panserin 401 medium (PAN-Biotech) containing 5% human male AB serum (Biowest), 100 U/ml penicillin, and 100 μg/ml streptomycin (Gibco). T cell blasts were expanded by incubating PBMCs for 72 h with 2.5 μg/ml phytohemagglutinin (Sigma-Aldrich); dead cells were then removed by Ficoll-Paque density-gradient (Lymphoprep; ProteoGenix) centrifugation; and T cell blasts were cultured in complete Panserin 401 culture medium supplemented with 100 IU/ml recombinant human IL-2 (R&D Systems). The Jurkat T cell line and Raji and Ramos B cell lines were cultured in complete RPMI 1640 GlutaMax medium (Invitrogen) containing 10% heat-inactivated FCS (Gibco), 100 U/ml penicillin, and 100 μg/ml streptomycin (Gibco). HEK293T cells, an SNK6 NK cell line, and LCLs were cultured in complete DMEM, high glucose, GlutaMAX supplement, and pyruvate medium (Gibco) containing 10% heat-inactivated fetal calf serum (Gibco), 100 U/ml penicillin, and 100 μg/ml streptomycin (Gibco). EBV-GFP+ HEK, double BZLF1-BRLF1-LCL1, and LCL2 cell lines have been described previously (Feederle et al., 2000; Delecluse et al., 1998).

Flow cytometry RNA assay
1.5 million to 3 million cells per well were washed in staining buffer (PBS-FCS 2%) before seeding in a 96-well round-bottomed plate. Membrane staining was performed before the PrimeFlow RNA assay for 30 min in the dark at 30°C in PBS-FCS 2%, followed by one washing step using PBS. A total of 1 μl/10^6 cells of membrane-targeting antibodies and 1:2,000 fixable viability dye eFluor 450 were used with PBS-FCS 2% in a total volume of 150 μl per well. For each type of sample, 10^6 cells were stained with eFluor 450, only to be used as positive and negative controls for EBER staining. Cell membrane staining without the PrimeFlow RNA assay was performed according to standard flow cytometry methods. The following validated antibodies were used: anti-CD2 (RPA-2.10), anti-CD3 (SK7), anti-CD4 (SK3 or OKT4), anti-CD5 (REA782), anti-CD8 (HIT8a or SKI1), anti-CD14 (M5E2), anti-CD16 (3G8), anti-CD19 (HIB19), anti-CD27 (LG.3A10), anti-CD38 (FUN-2), anti-CD45RA (HI100), anti-CD56 (B159 or 5.1H11), anti-CD57 (HNK-1), anti-CD80 (2D10), anti-CD107a (H4A3), anti-CD107b (H4B4), anti-CD160 (BY55), anti-CD226/DNAM-1 (TX25), anti-CD244/2B4 (C1.7), anti-CD335/NKp46 (9E2), anti-TCRδγ (REA591), anti-δ2 (REA771), anti-EOMES (WD1928), anti-IRF4 (IRF4.3E4), anti-Bcl-6 (IG191E/A8), anti-HLADR (L243), anti-IgD (IA6-2), anti-IgM (MHM-88), Tag-it Violet Proliferation and Cell Tracking Dye, and Fixable Viability Dye eFluor 450. These antibodies were conjugated to FITC, PE, PE-cyanine 5 (PE-Cy5), PE-Cy7, PE/Dazzle 594, allophycocyanin-Cy7, allophycocyanin-Vio7,

Brilliant Violet 421 (BV421), BV510, BV605, BV650, BV711, or BV785. RPL13A- and *Bacillus cereus*–specific probes (Alexa Fluor 488 [type 4, AF488] and Alexa Fluor 647 [type 1, AF647], respectively) were used as positive and negative control, respectively, for EBER probe staining in the same well stained only with eFluor 450. EBER target probe Alexa Fluor 647 (type 1, AF647) was used to stain EBV-infected cells previously stained with extracellular antibodies. Detection of *LMP1* and *EBNA2* transcripts was performed using Alexa Fluor 568 (type 10, AF568) probes designed to avoid strain sequence variations according to Feederle et al. (2015). The EBNA2 probe was a mixture of two probes targeting either type 1 or type 2 EBV. In situ hybridization for EBER, EBNA2, LMP1, RPL13A, and Bacillus was performed using probes and reagents supplied with the PrimeFlow RNA assay kit as described by the manufacturer (eBioscience).

Cytokine production assay
For intracellular staining of cytokines, T cell blasts were stimulated overnight with Dynabeads Human T-Activator CD3/CD28 (Invitrogen) or 1 µg/ml anti-CD3 antibody (clone OKT3; eBioscience) in the presence of brefeldin A (GolgiPlug; BD Biosciences). PBMCs from systemic CAEBV patients were thawed and processed without stimulation or brefeldin A. Cells were surface stained for CD3, CD4, CD8, or CD56 and CD16 before the PrimeFlow RNA assay was performed. Intracellular staining with PE-anti–IL-2 (rat IgG2a, MHQ1-17H12), BV711–anti–IFN-γ (mouse IgG1, 4S.B3), or PE-Cy–anti–TNF-α (mouse IgG1, Mab11) was performed after the permeabilization step according to the manufacturer's instructions. Analysis was performed by flow cytometry (LSR Fortessa X-20; BD Biosciences).

EBV-specific T cell detection
EBV-specific CD8^{+} T cells from PBMCs were detected using a mix of unlabeled EBV HLA-A2:01 Pro5 Pentamers (ProImmune) mixed with R-PE Pro5 Fluorotag in addition with BV785–anti–CD3, BV650-PE–anti–CD8, and BV510–anti–CD4 monoclonal antibodies. The EBV HLA-A2:01 Pro5 Pentamers mix contains four different pentamers presenting FLYALLALLL (residues 356–364 from LMP2), CLGGLLTMV (residues 426–434 from LMP2), GLCTLVAML (residues 259–267 from BMLF-1), or YLLEMLWRL (residues 125–133 from LMP1) peptide derived from LMP2, BMLF1, and LMP1 proteins of EBV. All staining was done according to the manufacturer's instructions. The PrimeFlow RNA assay was performed after these steps and before analysis by flow cytometry (LSR Fortessa X-20; BD Biosciences).

Proliferation assay
T cell blasts were washed and cultured without IL-2 for 72 h to synchronize the cells. T cell blasts or PBMCs were labeled with CellTrace Violet dye (Invitrogen) according to the manufacturer's instructions. Cells were then cultured for 3–7 d in complete Panserin 401 medium alone or in the presence of 0.1, 1, or 10 µg/ml immobilized anti-CD3 antibody (clone OKT3; eBioscience) and Dynabeads Human T-Activator CD3/CD28 (Invitrogen). Cells were surface stained for CD3, CD4, CD8, and HLA-DR detection, and the PrimeFlow RNA assay was

performed before analysis by flow cytometry (LSR Fortessa X-20; BD Biosciences). The proliferation index was calculated as previously described (Martin et al., 2014).

Degranulation assay
T cell blasts were stimulated for 3 h with 0.3, 3, and 30 µg/ml of immobilized anti-CD3 in the presence of PE-conjugated anti–LAMP-1/2 (H4A3, H4B4; BD Biosciences) as previously described (Martin et al., 2014). Cells were then washed and stained for surface expression of CD3, CD4, and CD8 before performing the PrimeFlow RNA assay and before analysis by flow cytometry (LSR Fortessa X-20; BD Biosciences).

Immunochemistry
Biopsies were fixed in 10% neutral buffered formalin, embedded in paraffin, and stained with hematoxylin-eosin. Immunohistochemical staining and in situ hybridization were performed on an automated stainer (BOND-MAX; Leica Biosystems). The presence of EBV was demonstrated by in situ hybridization with a probe for small RNA–encoding regions 1 and 2 (EBERs) probe (Dako). Antibodies used were anti-CD3 (polyclonal rabbit, CD3ε, A0452; Dako, Agilent Technologies), CD4 (monoclonal IgG1k mouse, NCL-L-CD4-368; Leica Biosystems), CD8 (monoclonal mouse IgG1k, C8/144B; Dako), CD20 (monoclonal mouse IgG2ak, L26; Dako), and anti-CD79a (monoclonal mouse IgG1k, JCB117; Dako).

RT-PCR for *BZLF1*
BZLF1 transcript expression was analyzed by semiquantitative PCR with the forward primer 5′-CATGTTTCAACCGCTCCGACT GG-3′ and the reverse primer 5′-TCACAGTTCACATCCTCCTTC TTC-3′ for *BZLF1* and with the forward primer 5′-GCGCAGCCT GTCATTTTCAGATG-3′ and the reverse primer 5′-CCTGCTTCA CCACCTTCTTG-3′ for *GAPDH* as a control for amplification and normalization.

Online supplemental material
Fig. S1 shows that the protocol conditions for the PrimeFlow EBER assay preserve extracellular staining for flow cytometry. Fig. S2 shows the background staining by the PrimeFlow assay obtained with a probe for Bacillus in patients with various EBV-driven LPDs. Fig. S3 shows the expression of NK cell markers in a patient with EBV[+] ENKTL (Pt 3.8) and immunostaining of tissue biopsies of patients with peripheral EBV[+] NK cell systemic CAEBV (Pt 6.2, 6.3, 6.8, and 6.9). Fig. S4 shows the detection of EBV^{+} B cells by the PrimeFlow EBER assay in a patient (Pt S4) with fulminant IM misdiagnosed as T/NK-LPD. Fig. S5 shows the detection of LMP1 and EBNA2 viral transcripts and intracellular cytokines by the PrimeFlow EBER assay.

References

Arai, A.. 2019. Advances in the study of chronic active Epstein-Barr virus infection: clinical features under the 2016 WHO classification and mechanisms of development. *Front Pediatr.* 7:14. https://doi.org/10.3389/fped.2019.00014

Babcock, G.J., L.L. Decker, R.B. Freeman, and D.A. Thorley-Lawson. 1999. Epstein-barr virus-infected resting memory B cells, not proliferating lymphoblasts, accumulate in the peripheral blood of immunosuppressed patients. *J. Exp. Med.* 190:567–576. https://doi.org/10.1084/jem.190.4.567

Balfour, H.H., Jr., C.J. Holman, K.M. Hokanson, M.M. Lelonek, J.E. Giesbrecht, D.R. White, D.O. Schmeling, C.-H. Webb, W. Cavert, D.H. Wang, et al. 2005. A prospective clinical study of Epstein-Barr virus and host interactions during acute infectious mononucleosis. *J. Infect. Dis.* 192: 1505–1512. https://doi.org/10.1086/491740

Bollard, C.M., and J.I. Cohen. 2018. How I treat T-cell chronic active Epstein-Barr virus disease. *Blood.* 131:2899–2905. https://doi.org/10.1182/blood-2018-03-785931

Chaganti, S., C.S. Ma, A.I. Bell, D. Croom-Carter, A.D. Hislop, S.G. Tangye, and A.B. Rickinson. 2008. Epstein-Barr virus persistence in the absence of conventional memory B cells: IgM+IgD+CD27+ B cells harbor the virus in X-linked lymphoproliferative disease patients. *Blood.* 112:672–679. https://doi.org/10.1182/blood-2007-10-116269

Chan, J.K., W.Y. Tsang, and C.S. Ng. 1996. Clarification of CD3 immunoreactivity in nasal T/natural killer cell lymphomas: the neoplastic cells are often CD3 epsilon+. *Blood.* 87:839–841. https://doi.org/10.1182/blood.V87.2.839.bloodjournal872839

Cohen, J.I., I. Manoli, K. Dowdell, T.A. Krogmann, D. Tamura, P. Radecki, W. Bu, S.-P. Turk, K. Liepshutz, R.L. Hornung, et al. 2019. Hydroa vacciniforme-like lymphoproliferative disorder: an EBV disease with a low risk of systemic illness in whites. *Blood.* 133:2753–2764. https://doi.org/10.1182/blood.2018893750

Delecluse, H.-J., T. Hilsendegen, D. Pich, R. Zeidler, and W. Hammerschmidt. 1998. Propagation and recovery of intact, infectious Epstein-Barr virus from prokaryotic to human cells. *Proc. Natl. Acad. Sci. USA.* 95: 8245–8250. https://doi.org/10.1073/pnas.95.14.8245

Feederle, R., M. Kost, M. Baumann, A. Janz, E. Drouet, W. Hammerschmidt, and H.-J. Delecluse. 2000. The Epstein-Barr virus lytic program is controlled by the co-operative functions of two transactivators. *EMBO J.* 19:3080–3089. https://doi.org/10.1093/emboj/19.12.3080

Feederle, R., O. Klinke, A. Kutikhin, R. Poirey, M.-H. Tsai, and H.-J. Delecluse. 2015. Epstein-Barr virus: from the detection of sequence polymorphisms to the recognition of viral types. *Curr. Top. Microbiol. Immunol.* 390:119–148. https://doi.org/10.1007/978-3-319-22822-8_7

Gilligan, K., P. Rajadurai, L. Resnick, and N. Raab-Traub. 1990. Epstein-Barr virus small nuclear RNAs are not expressed in permissively infected cells in AIDS-associated leukoplakia. *Proc. Natl. Acad. Sci. USA.* 87: 8790–8794. https://doi.org/10.1073/pnas.87.22.8790

Greifenegger, N., M. Jäger, L.A. Kunz-Schughart, H. Wolf, and F. Schwarzmann. 1998. Epstein-Barr virus small RNA (EBER) genes: differential regulation during lytic viral replication. *J. Virol.* 72:9323–9328. https://doi.org/10.1128/JVI.72.11.9323-9328.1998

Hadinoto, V., M. Shapiro, T.C. Greenough, J.L. Sullivan, K. Luzuriaga, and D.A. Thorley-Lawson. 2008. On the dynamics of acute EBV infection and the pathogenesis of infectious mononucleosis. *Blood.* 111:1420–1427. https://doi.org/10.1182/blood-2007-06-093278

Henning, A.L., J.N.B. Sampson, and B.K. McFarlin. 2016. Measurement of low-abundance intracellular mRNA using amplified FISH staining and image-based flow cytometry. *Curr. Protoc. Cytom.* 76:1–: 8. https://doi.org/10.1002/0471142956.cy0746s76

Hochberg, D., T. Souza, M. Catalina, J.L. Sullivan, K. Luzuriaga, and D.A. Thorley-Lawson. 2004. Acute infection with Epstein-Barr virus targets and overwhelms the peripheral memory B-cell compartment with resting, latently infected cells. *J. Virol.* 78:5194–5204. https://doi.org/10.1128/JVI.78.10.5194-5204.2004

Hohaus, S., R. Santangelo, M. Giachelia, B. Vannata, G. Massini, A. Cuccaro, M. Martini, V. Cesarini, T. Cenci, F. D'Alo, et al. 2011. The viral load of Epstein-Barr virus (EBV) DNA in peripheral blood predicts for biological and clinical characteristics in Hodgkin lymphoma. *Clin. Cancer Res.* 17:2885–2892. https://doi.org/10.1158/1078-0432.CCR-10-3327

Hu, B., and Y. Oki. 2018. Novel immunotherapy options for extranodal NK/T-cell lymphoma. *Front. Oncol.* 8:139. https://doi.org/10.3389/fonc.2018.00139

Hue, S.S., M.L. Oon, S. Wang, S.Y. Tan, and S.B. Ng. 2020. Epstein-Barr virus-associated T- and NK-cell lymphoproliferative diseases: an update and diagnostic approach. *Pathology.* 52:111–127. https://doi.org/10.1016/j.pathol.2019.09.011

Ingham, R.J., J. Raaijmakers, C.S.H. Lim, G. Mbamalu, G. Gish, F. Chen, L. Matskova, I. Ernberg, G. Winberg, and T. Pawson. 2005. The Epstein-Barr virus protein, latent membrane protein 2A, co-opts tyrosine kinases used by the T cell receptor. *J. Biol. Chem.* 280:34133–34142. https://doi.org/10.1074/jbc.M507831200

Ito, T., H. Kawazu, T. Murata, S. Iwata, S. Arakawa, Y. Sato, K. Kuzushima, F. Goshima, and H. Kimura. 2014. Role of latent membrane protein 1 in chronic active Epstein-Barr virus infection-derived T/NK-cell proliferation. *Cancer Med.* 3:787–795. https://doi.org/10.1002/cam4.256

Iwata, S., K. Wada, S. Tobita, K. Gotoh, Y. Ito, A. Demachi-Okamura, N. Shimizu, Y. Nishiyama, and H. Kimura. 2010. Quantitative analysis of Epstein-Barr virus (EBV)-related gene expression in patients with chronic active EBV infection. *J. Gen. Virol.* 91:42–50. https://doi.org/10.1099/vir.0.013482-0

Izawa, K., E. Martin, C. Soudais, J. Bruneau, D. Boutboul, R. Rodriguez, C. Lenoir, A.D. Hislop, C. Besson, F. Touzot, et al. 2017. Inherited CD70 deficiency in humans reveals a critical role for the CD70-CD27 pathway in immunity to Epstein-Barr virus infection. *J. Exp. Med.* 214:73–89. https://doi.org/10.1084/jem.20160784

Joly, E., and D. Hudrisier. 2003. What is trogocytosis and what is its purpose? *Nat. Immunol.* 4:815. https://doi.org/10.1038/ni0903-815

Kassambara, A., T. Rème, M. Jourdan, T. Fest, D. Hose, K. Tarte, and B. Klein. 2015. GenomicScape: an easy-to-use web tool for gene expression data analysis. Application to investigate the molecular events in the differentiation of B cells to plasma cells. *PLOS Comput. Biol.* 11. e1004077. https://doi.org/10.1371/journal.pcbi.1004077

Kawabe, S., Y. Ito, K. Gotoh, S. Kojima, K. Matsumoto, T. Kinoshita, S. Iwata, Y. Nishiyama, and H. Kimura. 2012. Application of flow cytometric in situ hybridization assay to Epstein-Barr virus-associated T/natural killer cell lymphoproliferative diseases. *Cancer Sci.* 103:1481–1488. https://doi.org/10.1111/j.1349-7006.2012.02305.x

Kawamoto, K., H. Miyoshi, T. Suzuki, Y. Kozai, K. Kato, M. Miyahara, T. Yujiri, I. Choi, K. Fujimaki, T. Muta, et al. 2018. A distinct subtype

of Epstein-Barr virus-positive T/NK-cell lymphoproliferative disorder: adult patients with chronic active Epstein-Barr virus infection-like features. *Haematologica*. 103:1018–1028. https://doi.org/10.3324/haematol.2017.174177

Kim, S.J., D.H. Yoon, A. Jaccard, W.J. Chng, S.T. Lim, H. Hong, Y. Park, K.M. Chang, Y. Maeda, F. Ishida, et al. 2016. A prognostic index for natural killer cell lymphoma after non-anthracycline-based treatment: a multicentre, retrospective analysis. *Lancet Oncol.* 17:389–400. https://doi.org/10.1016/S1470-2045(15)00533-1

Kim, W.Y., I.A. Montes-Mojarro, F. Fend, and L. Quintanilla-Martinez. 2019. Epstein-Barr virus-associated T and NK-cell lymphoproliferative diseases. *Front Pediatr.* 7:71. https://doi.org/10.3389/fped.2019.00071

Kimura, H., and Y.-L. Kwong. 2019. EBV viral loads in diagnosis, monitoring, and response assessment. *Front. Oncol.* 9:62. https://doi.org/10.3389/fonc.2019.00062

Kimura, H., K. Miyake, Y. Yamauchi, K. Nishiyama, S. Iwata, K. Iwatsuki, K. Gotoh, S. Kojima, Y. Ito, and Y. Nishiyama. 2009. Identification of Epstein-Barr virus (EBV)-infected lymphocyte subtypes by flow cytometric in situ hybridization in EBV-associated lymphoproliferative diseases. *J. Infect. Dis.* 200:1078–1087. https://doi.org/10.1086/605610

Kimura, H., Y. Ito, S. Kawabe, K. Gotoh, Y. Takahashi, S. Kojima, T. Naoe, S. Esaki, A. Kikuta, A. Sawada, et al. 2012. EBV-associated T/NK-cell lymphoproliferative diseases in nonimmunocompromised hosts: prospective analysis of 108 cases. *Blood.* 119:673–686. https://doi.org/10.1182/blood-2011-10-381921

Laichalk, L.L., D. Hochberg, G.J. Babcock, R.B. Freeman, and D.A. Thorley-Lawson. 2002. The dispersal of mucosal memory B cells: evidence from persistent EBV infection. *Immunity.* 16:745–754. https://doi.org/10.1016/S1074-7613(02)00318-7

Latour, S., and A. Fischer. 2019. Signaling pathways involved in the T-cell-mediated immunity against Epstein-Barr virus: Lessons from genetic diseases. *Immunol. Rev.* 291:174–189. https://doi.org/10.1111/imr.12791

Latour, S., and S. Winter. 2018. Inherited immunodeficiencies with high predisposition to Epstein-Barr virus-driven lymphoproliferative diseases. *Front. Immunol.* 9:1103. https://doi.org/10.3389/fimmu.2018.01103

Lee, J.H., J. Choi, Y.-O. Ahn, T.M. Kim, and D.S. Heo. 2018. CD21-independent Epstein-Barr virus entry into NK cells. *Cell. Immunol.* 327:21–25. https://doi.org/10.1016/j.cellimm.2018.01.011

Lerner, M.R., N.C. Andrews, G. Miller, and J.A. Steitz. 1981. Two small RNAs encoded by Epstein-Barr virus and complexed with protein are precipitated by antibodies from patients with systemic lupus erythematosus. *Proc. Natl. Acad. Sci. USA.* 78:805–809. https://doi.org/10.1073/pnas.78.2.805

Li, F.-Y., B. Chaigne-Delalande, C. Kanellopoulou, J.C. Davis, H.F. Matthews, D.C. Douek, J.I. Cohen, G. Uzel, H.C. Su, and M.J. Lenardo. 2011. Second messenger role for Mg^{2+} revealed by human T-cell immunodeficiency. *Nature.* 475:471–476. https://doi.org/10.1038/nature10246

Li, Z., M.-H. Tsai, A. Shumilov, F. Baccianti, S.W. Tsao, R. Poirey, and H.-J. Delecluse. 2019. Epstein-Barr virus ncRNA from a nasopharyngeal carcinoma induces an inflammatory response that promotes virus production. *Nat. Microbiol.* 4:2475–2486. https://doi.org/10.1038/s41564-019-0546-y

Ma, C.S., S. Pittaluga, D.T. Avery, N.J. Hare, I. Maric, A.D. Klion, K.E. Nichols, and S.G. Tangye. 2006. Selective generation of functional somatically mutated IgM^+CD27^+, but not Ig isotype-switched, memory B cells in X-linked lymphoproliferative disease. *J. Clin. Invest.* 116:322–333. https://doi.org/10.1172/JCI25720

Martin, E., N. Palmic, S. Sanquer, C. Lenoir, F. Hauck, C. Mongellaz, S. Fabrega, P. Nitschké, M.D. Esposti, J. Schwartzentruber, et al. 2014. CTP synthase 1 deficiency in humans reveals its central role in lymphocyte proliferation. *Nature.* 510:288–292. https://doi.org/10.1038/nature13386

Martin, E., N. Minet, A.-C. Boschat, S. Sanquer, S. Sobrino, C. Lenoir, J.P. de Villartay, M. Leite-de-Moraes, C. Picard, C. Soudais, et al; Genomics England Research Consortium. 2020. Impaired lymphocyte function and differentiation in CTPS1-deficient patients result from a hypomorphic homozygous mutation. *JCI Insight.* 5.133880. https://doi.org/10.1172/jci.insight.133880

McHugh, D., N. Caduff, M.H.M. Barros, P.C. Rämer, A. Raykova, A. Murer, V. Landtwing, I. Quast, C.T. Styles, M. Spohn, et al. 2017. Persistent KSHV infection increases EBV-associated tumor formation *in vivo* via enhanced EBV lytic gene expression. *Cell Host Microbe.* 22:61–73.e7. https://doi.org/10.1016/j.chom.2017.06.009

Okuno, Y., T. Murata, Y. Sato, H. Muramatsu, Y. Ito, T. Watanabe, T. Okuno, N. Murakami, K. Yoshida, A. Sawada, et al. 2019. Defective Epstein-Barr virus in chronic active infection and haematological malignancy. *Nat. Microbiol.* 4:404–413. https://doi.org/10.1038/s41564-018-0334-0

Pekalski, M.L., A.R. García, R.C. Ferreira, D.B. Rainbow, D.J. Smyth, M. Mashar, J. Brady, N. Savinykh, X.C. Dopico, S. Mahmood, et al. 2017. Neonatal and adult recent thymic emigrants produce IL-8 and express complement receptors CR1 and CR2. *JCI Insight.* 2:93739. https://doi.org/10.1172/jci.insight.93739

Plummer, M., C. de Martel, J. Vignat, J. Ferlay, F. Bray, and S. Franceschi. 2016. Global burden of cancers attributable to infections in 2012: a synthetic analysis. *Lancet Glob. Health.* 4:e609–e616. https://doi.org/10.1016/S2214-109X(16)30143-7

Quintanilla-Martinez, L., C. Ridaura, F. Nagl, M. Sáez-de-Ocariz, C. Durán-McKinster, R. Ruiz-Maldonado, G. Alderete, P. Grube, C. Lome-Maldonado, I. Bonzheim, et al. 2013. Hydroa vacciniforme-like lymphoma: a chronic EBV+ lymphoproliferative disorder with risk to develop a systemic lymphoma. *Blood.* 122:3101–3110. https://doi.org/10.1182/blood-2013-05-502203

Rodriguez, R., B. Fournier, D.J. Cordeiro, S. Winter, K. Izawa, E. Martin, D. Boutboul, C. Lenoir, S. Fraitag, S. Kracker, et al. 2019. Concomitant *PIK3CD* and *TNFRSF9* deficiencies cause chronic active Epstein-Barr virus infection of T cells. *J. Exp. Med.* 216:2800–2818. https://doi.org/10.1084/jem.20190678

Ryan, J.L., H. Fan, L.J. Swinnen, S.A. Schichman, N. Raab-Traub, M. Covington, S. Elmore, and M.L. Gulley. 2004. Epstein-Barr Virus (EBV) DNA in plasma is not encapsidated in patients with EBV-related malignancies. *Diagn. Mol. Pathol.* 13:61–68. https://doi.org/10.1097/00019606-200406000-00001

Sawada, A., and M. Inoue. 2018. Hematopoietic stem cell transplantation for the treatment of Epstein-Barr virus-associated T- or NK-cell lymphoproliferative diseases and associated disorders. *Front Pediatr.* 6:334. https://doi.org/10.3389/fped.2018.00334

Sawada, A., M. Inoue, and K. Kawa. 2017. How we treat chronic active Epstein-Barr virus infection. *Int. J. Hematol.* 105:406–418. https://doi.org/10.1007/s12185-017-2192-6

Swerdlow, S.H., E. Campo, S.A. Pileri, N.L. Harris, H. Stein, R. Siebert, R. Advani, M. Ghielmini, G.A. Salles, A.D. Zelenetz, et al. 2016. The 2016 revision of the World Health Organization classification of lymphoid neoplasms. *Blood.* 127:2375–2390. https://doi.org/10.1182/blood-2016-01-643569

Tabiasco, J., A. Vercellone, F. Meggetto, D. Hudrisier, P. Brousset, and J.-J. Fournié. 2003. Acquisition of viral receptor by NK cells through immunological synapse. *J. Immunol.* 170:5993–5998. https://doi.org/10.4049/jimmunol.170.12.5993

Tangye, S.G., U. Palendira, and E.S.J. Edwards. 2017. Human immunity against EBV-lessons from the clinic. *J. Exp. Med.* 214:269–283. https://doi.org/10.1084/jem.20161846

Thorley-Lawson, D.A., and G.J. Babcock. 1999. A model for persistent infection with Epstein-Barr virus: the stealth virus of human B cells. *Life Sci.* 65:1433–1453. https://doi.org/10.1016/S0024-3205(99)00214-3

Thorley-Lawson, D.A., J.B. Hawkins, S.I. Tracy, and M. Shapiro. 2013. The pathogenesis of Epstein-Barr virus persistent infection. *Curr. Opin. Virol.* 3:227–232. https://doi.org/10.1016/j.coviro.2013.04.005

Tierney, R.J., C.D. Shannon-Lowe, L. Fitzsimmons, A.I. Bell, and M. Rowe. 2015. Unexpected patterns of Epstein-Barr virus transcription revealed by a high throughput PCR array for absolute quantification of viral mRNA. *Virology.* 474:117–130. https://doi.org/10.1016/j.virol.2014.10.030

Young, L.S., and A.B. Rickinson. 2004. Epstein-Barr virus: 40 years on. *Nat. Rev. Cancer.* 4:757–768. https://doi.org/10.1038/nrc1452

Zhang, P., C. Zeng, J. Cheng, J. Zhou, J. Gu, X. Mao, W. Zhang, Y. Cao, H. Luo, B. Xu, et al. 2019. Determination of Epstein-Barr virus-infected lymphocyte cell types in peripheral blood mononuclear cells as a valuable diagnostic tool in hematological diseases. *Open Forum Infect. Dis.* 6. ofz171. https://doi.org/10.1093/ofid/ofz171
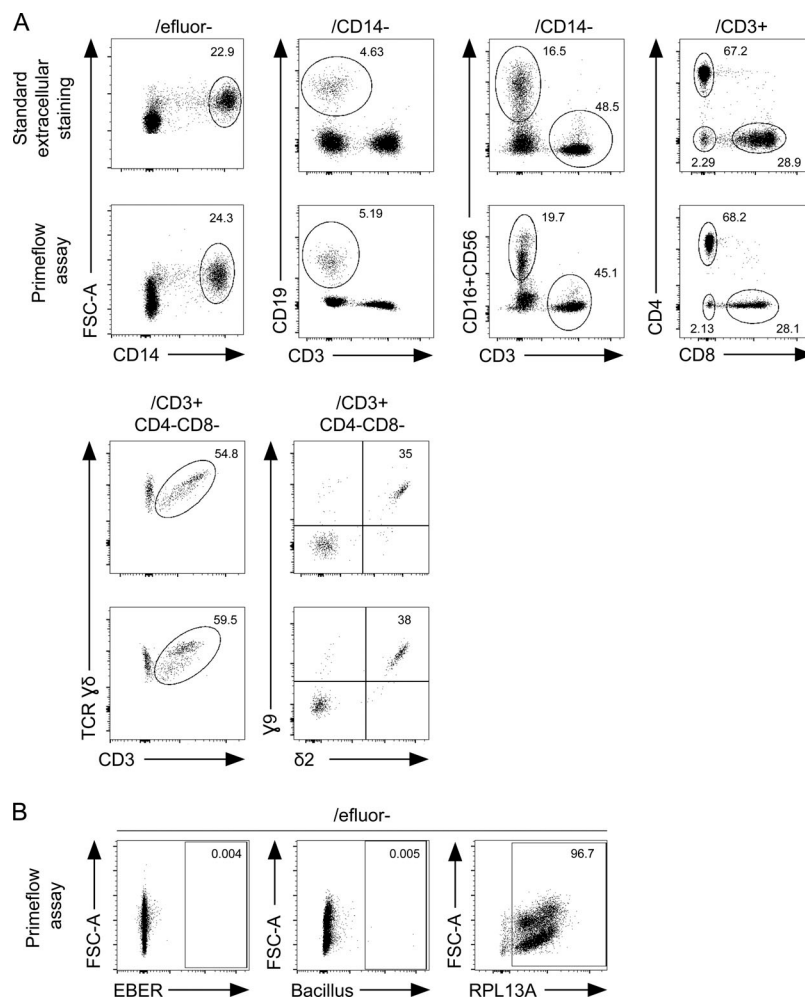
Figure S1. **Conservation of extracellular staining in PrimeFlow EBER assay conditions. (A)** FACS dot plots for common extracellular markers (CD3, CD4, CD8, CD14, CD19, CD16, CD56, γδ TCR, Vδ2 TCR, and Vγ9 TCR) from PBMCs of a healthy donor using a conventional staining protocol (upper panels) compared with protocol conditions of the PrimeFlow EBER assay (lower panels). **(B)** FACS dot plots of EBERs (lane 1), Bacillus (lane 2), and RPL13A (lane 3) expression from PBMCs of the same healthy donor as in A using the PrimeFlow RNA assay.
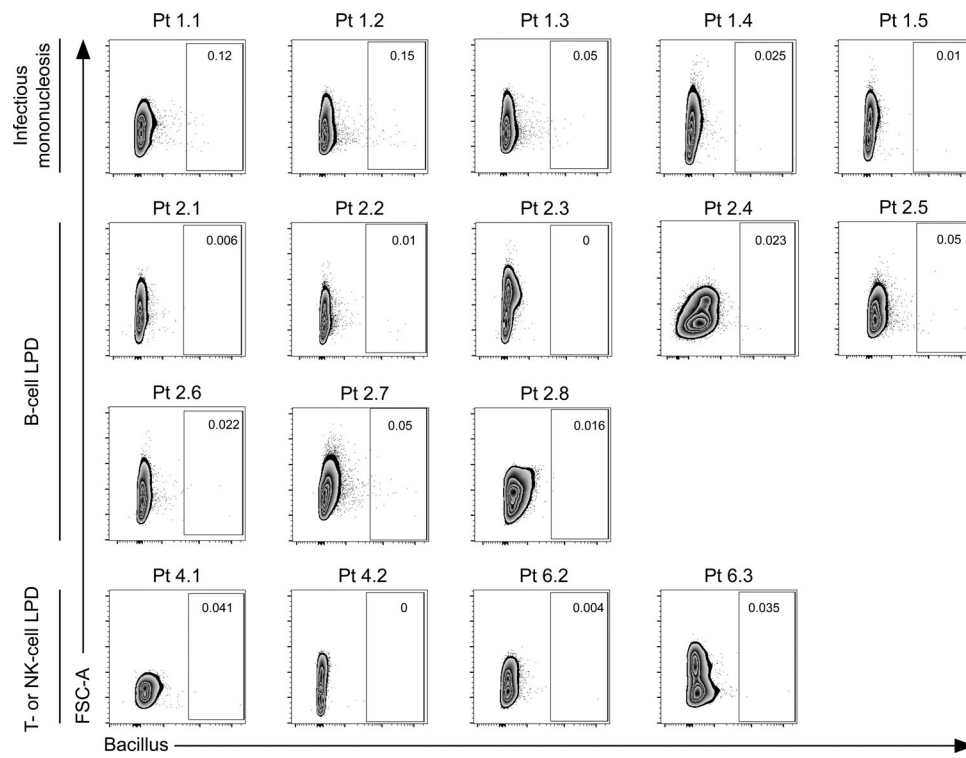
Figure S2. **Control Bacillus staining by PrimeFlow assay in patients with various EBV-driven LPDs.** FACS dot plots of Bacillus staining using the PrimeFlow RNA assay of PBMCs from patients with IM from Fig. 1 B (upper panels), EBV+ B cell LPDs from Fig. 2 (middle panels), and EBV+ T or NK cell LPDs from Fig. 4 and Fig. 6 (lower panels).
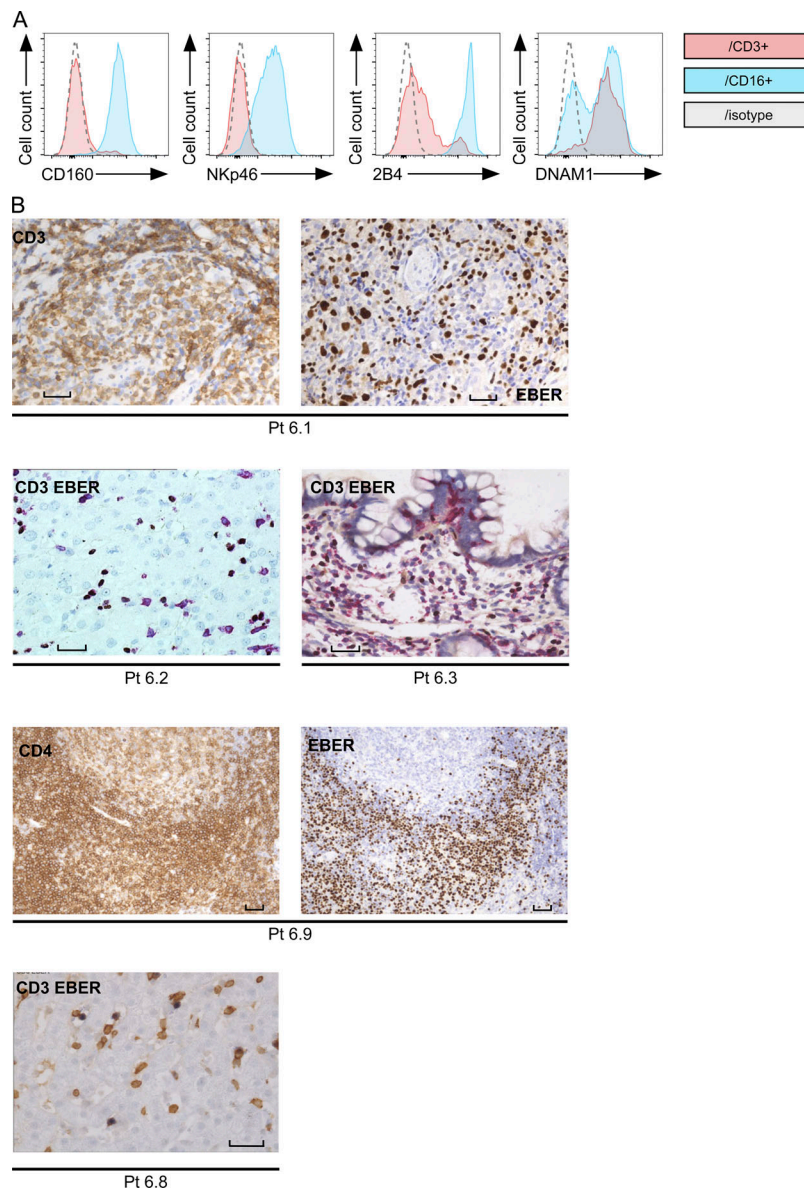
Figure S3. Expression of NK cell markers in a patient (Pt. 3.8) with EBV⁺ ENKTL T/NK lymphoma and immunostaining from tissue biopsies of patients with peripheral EBV⁺ NK cell systemic CAEBV. (A) FACS histograms with anti-CD160, anti-NKp46, anti-2B4, anti-DNAM1, or isotype staining gated on CD3⁺ or CD16⁺ cells from PBMCs of Pt 3.8 shown in Fig. 3 C. **(B)** Skin biopsy from Pt 6.1 with anti-CD3ε or EBER probe staining (magnification, ×400), liver biopsy from Pt 6.2 with anti-CD3ε and EBER probe costaining (magnification, ×400), and gut biopsy from Pt 6.3 with anti-CD3ε and EBER probe costaining (magnification, ×400), showing infiltration of EBV-infected T cells. Liver biopsy from Pt 6.8 with anti-CD3ε and EBER costaining (magnification, ×400). Mouth tumor biopsy from Pt 6.9 with CD4 or EBER staining (magnification, ×200). Scale bars, 40 µm. All show T cell infiltration in tissues.
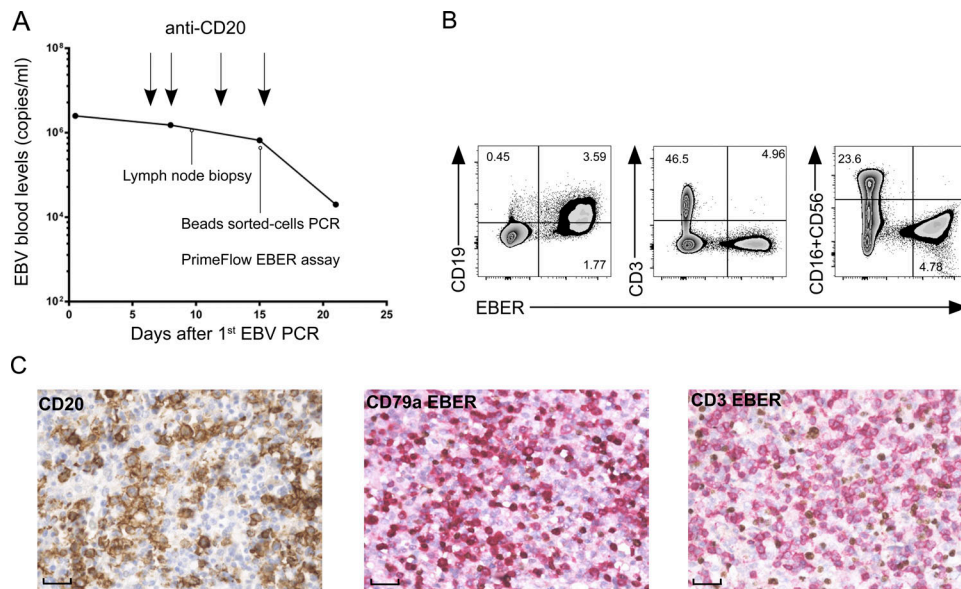
Figure S4. Detection of EBV⁺ B cells by PrimeFlow EBER assay in a patient (Pt S4) with fulminant IM misdiagnosed as T/NK-LPD. (A) EBV blood loads with EBV copies at different time points (black circles). Arrows indicate anti-CD20 antibody infusions. Times of investigations (lymph node biopsy, beads, sorted cells for EBV PCR, PrimeFlow EBER assay) for diagnosis are also indicated. **(B)** FACS dot plots of EBER expression by PrimeFlow assay coupled with staining for CD19, CD3, CD16, and CD56 from PBMCs after anti-CD20 infusions. At that time, no B cells were detected in the periphery, and EBV load on sorted T cells was positive. **(C)** Lymph node biopsy with anti-CD20 staining, anti-CD79a and EBER probe costaining, and anti-CD3ε and EBER probe costaining. Magnification, ×400. Scale bars, 40 µm.
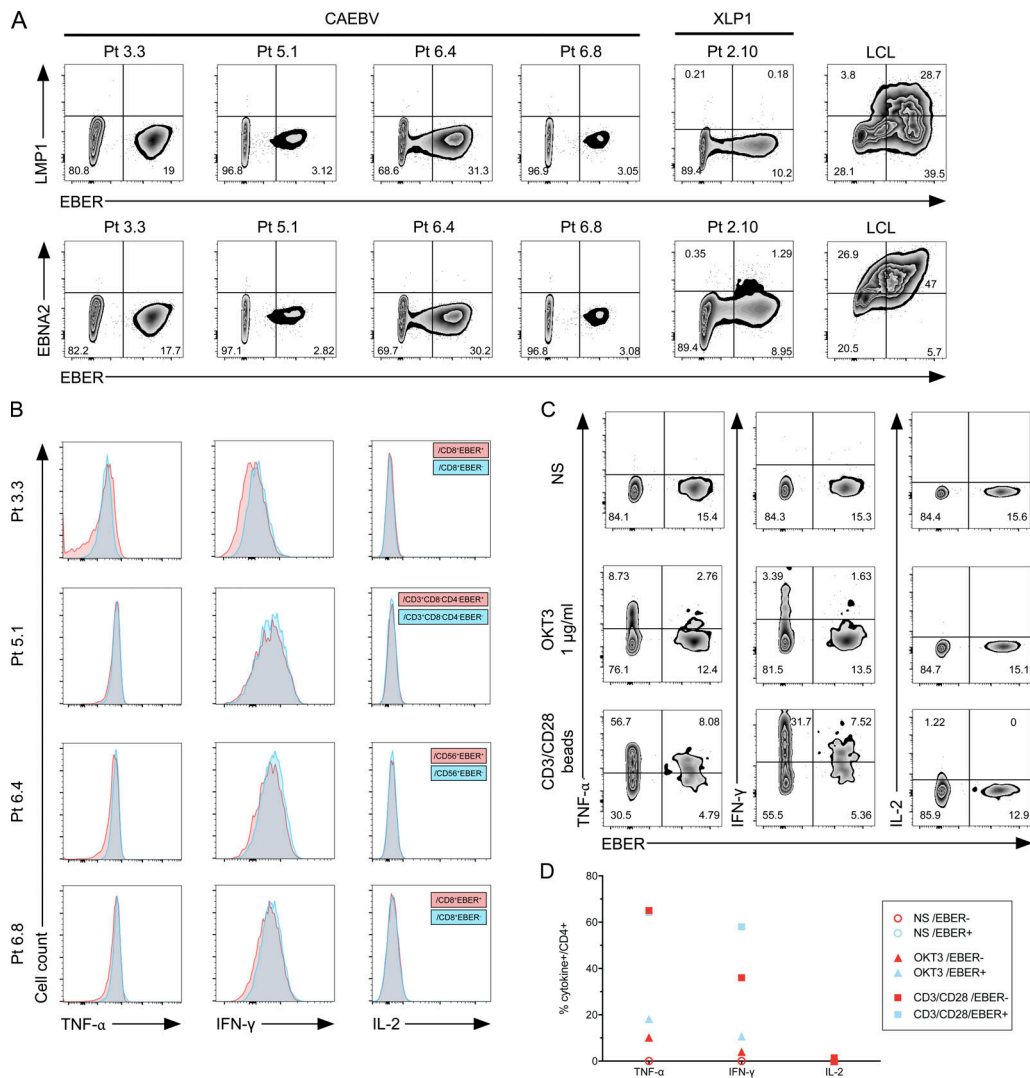
Figure S5. **Detection of LMP1 and EBNA2 viral transcripts and intracellular cytokines by PrimeFlow EBER assay. (A)** FACS dot plots of LMP1 and EBER transcript coexpression by PrimeFlow assay in PBMCs from CAEBV and XLP1 patients and one LCL are shown in the upper panels. FACS dot plots of EBNA2 and EBER transcript coexpression by PrimeFlow assay are shown in the lower panels. Dot plots are gated on eFluor⁻ cells. The first digit of patient identification indicates the number of the figure in which it is presented in the main article. **(B)** FACS histograms of TNF-α, IFN-γ, and IL-2 intracellular detection gated on EBER⁺ or EBER⁻ CD4, CD8, CD3, or CD56 cell subsets from unstimulated PBMCs of four CAEBV patients. For each patient, the EBV-infected subset is indicated in the panels for IL-2 staining. **(C)** FACS dot plots of TNF-α, IFN-γ, IL-2, and EBER intracellular detection gated on CD4⁺ T cell blasts of the CAEBV patient Pt S5 (see Table 1). T cell blasts were stimulated or not with 1 µg/ml of anti-CD3 (OKT3) or anti-CD3/CD28 beads for 12 h. **(D)** Graphed data from the experiment shown in C.

Table S1 is provided online and lists antibodies and oligonucleotide probes tested in with PrimeFlow RNA assay.